

## Seismic hazard assessment of the Kivu rift segment based on a new seismotectonic zonation model (western branch, East African Rift system)

Damien Delvaux <sup>a,\*</sup>, Jean-Luc Mulumba <sup>b</sup>, Mwene Ntabwoba Stanislas Sebagenzi <sup>b</sup>, Silvanos Fiamma Bondo <sup>c</sup>, François Kervyn <sup>a</sup>, Hans-Balder Havenith <sup>d</sup>

<sup>a</sup> Royal Museum of Central Africa, Dept. of Earth Sciences, Belgium

<sup>b</sup> University of Lubumbashi, Dept. of Geology, Lubumbashi, DR, Congo

<sup>c</sup> Centre de Recherche en Sciences Naturelles (CRSN), Dept. of Geophysics, Lwiro, DR, Congo

<sup>d</sup> University of Liège, Dept. of Geology, Liège, Belgium



### ARTICLE INFO

#### Article history:

Received 9 October 2015

Received in revised form

1 August 2016

Accepted 18 October 2016

Available online 22 October 2016

#### Keywords:

Kivu rift

Neotectonic map

Seismotectonic zonation

Earthquake catalogue

Probabilistic seismic hazard assessment

### ABSTRACT

In the frame of the Belgian GeoRisCA multi-risk assessment project focusing on the Kivu and northern Tanganyika rift region in Central Africa, a new probabilistic seismic hazard assessment has been performed for the Kivu rift segment in the central part of the western branch of the East African rift system. As the geological and tectonic setting of this region is incompletely known, especially the part lying in the Democratic Republic of the Congo, we compiled homogeneous cross-border tectonic and neotectonic maps.

The seismic risk assessment is based on a new earthquake catalogue based on the ISC reviewed earthquake catalogue and supplemented by other local catalogues and new macroseismic epicenter data spanning 126 years, with 1068 events. The magnitudes have been homogenized to Mw and aftershocks removed. The final catalogue used for the seismic hazard assessment spans 60 years, from 1955 to 2015, with 359 events and a magnitude of completeness of 4.4. The seismotectonic zonation into 7 seismic source areas was done on the basis of the regional geological structure, neotectonic fault systems, basin architecture and distribution of thermal springs and earthquake epicenters.

The Gutenberg-Richter seismic hazard parameters were determined by the least square linear fit and the maximum likelihood method. Seismic hazard maps have been computed using existing attenuation laws with the Crisis 2012 software. We obtained higher PGA values (475 years return period) for the Kivu rift region than the previous estimates. They also vary laterally in function of the tectonic setting, with the lowest value in the volcanically active Virunga – Rutshuru zone, highest in the currently non-volcanic parts of Lake Kivu, Rusizi valley and North Tanganyika rift zone, and intermediate in the regions flanking the axial rift zone.

© 2016 Elsevier Ltd. All rights reserved.

## 1. Introduction

The Kivu rift region in the Great Lakes region of Central Africa has been recognised as seismically active as early as in the first half of the 20th century by the first explorers who reported a series of felt earthquakes (Cornet, 1910; Passau, 1911, 1912; Krenkel, 1922; Sieberg, 1932). It was included in the map of seismic areas of the East African rift of Willis (1936). Herrinck (1959), using a data base

of felt seisms recorded at meteorological stations, produced a map of density showing the felt earthquakes per square degree in which the Kivu rift region appears as the most seismically active part.

In the 1950's, the '*Institut pour la Recherche en Afrique centrale*' (IRSAC) installed the first regional seismic network in Central Africa, centred on the Lwiro research center along the southwestern shore of Lake Kivu (De Bremaecker, 1956, 1959; 1961). The latter, together with Sutton and Berg (1958), used the first seismological data from the IRSAC network to characterise the local seismicity. Wohlenberg (1968, 1969) exploited the available seismic data and produced an instrumental catalogue for the period 1956–1963.

\* Corresponding author.

E-mail address: [damien.delvaux@africamuseum.be](mailto:damien.delvaux@africamuseum.be) (D. Delvaux).

Some of these events have been revised by Turyomurugyendo (1996) during the compilation of the Global Seismic Hazard Assessment Program (GSHAP) seismic catalogue for East Africa (Giardini, 1999).

In 1992, Zana et al. (1992) estimated the earthquake hazard for the Kivu rift region for 1909–1980 and issued a map of earthquake risk in terms of equivalent earthquake magnitude distribution. Using the revised catalogue of Turyomurugyendo (1996) for East Africa, this region was included in one seismic source zone of the seismic hazard assessment map for Eastern and Southern Africa produced by Midzi et al. (1999). It was also considered by Mavonga and Durrheim (2009) in their probabilistic seismic hazard assessment for the Democratic Republic of Congo (DRC) and surrounding areas. Kijko (2008) also produced a probabilistic seismic hazard map for Sub-Saharan Africa as an application of a new calculation procedure.

The main problems encountered in the existing seismic hazard assessments for Central Africa are the heterogeneity and incompleteness of the catalogues, the short period of the instrumental recording, the poor knowledge of the active tectonics, the absence of detailed paleoseismic studies of active faults and the arbitrary definition of the seismic source zones. However, this highly populated region is increasingly at risk due to fast demographic growth, coupled with poor infrastructure and the absence or lack of enforcement of building code. Within this work, we aim at revising the seismic hazard assessment for the Kivu rift region, using a revised and longer database of seismicity (60 years) and more realistic seismotectonic source zones, with a probabilistic approach. This work was performed in the frame of the GeoRisCA project (Georisks in Central Africa) of the Belgian Federal Science Policy and also as a contribution to the IGGP 601 project “Seismotectonics and seismic hazards of Africa” and the Seismotectonic Map of Africa (Meghraoui et al., 2016).

As the geological knowledge of the Kivu rift region is incomplete and fragmentary, without synthetic geological maps across the political borders, we first compiled a homogeneous geological and structural map across the five countries of the Kivu rift region, mapped the Late Quaternary faults and compiled the existing knowledge on the thermal springs (assumed to be diagnostic of current tectonic activity along faults) in order to produce new geological and neotectonic maps for the region. The seismotectonic characteristics of the region (stress field, depth of faulting) were revised using published focal mechanism data and the neotectonic faults are analyzed using the empirical magnitude-length relations.

A new catalogue of instrumental and historical seismicity was compiled and processed in order to remove duplicates, homogenize the magnitudes and decluster it by removing the dependent shocks. The seismic source zones are defined on the basis of the new geological and neotectonic maps and the pattern of seismicity. The Gutenberg-Richter parameters and maximum regional magnitudes are determined using both the classical least square linear regression and the maximum likelihood method (Kijko and Smit, 2012). With a selection of three existing attenuation laws appropriate for the study region, probabilistic seismic hazard maps were computed using the CRISIS 2012 software (Ordaz et al., 2013). The results are compared with the previous estimations of peak ground accelerations and the uncertainties associated with the entire process discussed. Implications in terms of seismic hazard are discussed with special attention to the main large cities in the region.

The areal extent ( $0^{\circ}\text{S}$ – $5^{\circ}\text{S}$ ;  $27^{\circ}\text{E}$ – $32^{\circ}\text{E}$ ) was defined larger than the seismic hazard map (Fig. 1) in order to limit boundary effects of the seismic hazard assessment (decreasing hazard towards the borders) for the target area.

## 2. Geological and tectonic setting

The Kivu rift region lies in the central part of the western branch of the East African rift system (Ebinger, 1989a) which is considered in an early continental extension stage (Déprez et al., 2013). It extends over Rwanda, Burundi, eastern Democratic Republic of Congo (DRC), SW Uganda and NW Tanzania (Fig. 1). It developed in the Mesoproterozoic Karagwe-Ankolean belt (formerly Kibaran belt) and the Paleoproterozoic Rusizian belt (extension of the Ubendian Belt known in Tanzania, to the DRC side), which lie between the Congo and Tanzanian cratons (Tack et al., 2010; Fernandez et al., 2012). Rifting in this region started at about 11 Ma (Ebinger, 1989b; Pasteels et al., 1989; Kampunzu et al., 1998; Pouclet et al., 2016) as a consequence of the divergence between the Nubia and the Victoria plate. The Kivu rift opens at about 2 mm/yr (Saria et al., 2014) in a direction sub-orthogonal to the rift axis and in a dominant normal faulting regime (Tanaka et al., 1980; Delvaux and Barth, 2010).

### 2.1. Basement geology

The Precambrian basement is relatively well known on the eastern side of the Kivu rift, in Rwanda, Burundi, SW Uganda and NW Tanzania, but only the geological synthetic map of Lepersonne (1974) at 1/2.000.000 scale exists on the DRC side, based on old, preliminary and fragmentary maps. We compiled a general map by integrating data from various geological maps at different scales, publications and reports. We used the geological maps of Salée et al. (1939), and BRGM (1982) for the DRC, and Fernandez-Alonso (2007) for the Rwanda, Burundi, Tanzania and Uganda parts. The stratigraphy, magmatism and tectonics was synthesized from Cahen (1976), Cahen et al. (1979), Lepersonne (1974), Lavreau (1977), Walemba and Master (2005), Tack et al. (2010) and Fernandez et al. (2012). This was complemented by results from local field and/or remote-sensing studies of Passau (1932), Villeneuve (1976, 1977), Biayi-Kalala (1984), Kampunzu et al. (1985, 1998), Lubala et al. (1986), Rumvegeri (1987, 1991), Waleffe (1988), Ladmirand and Waleffe (1991), Brinckmann et al. (2001), Lefévére (2003) and Villeneuve and Guyonnet-Benaize (2006). This compilation provides a new and homogeneous view of the Precambrian basement structure across the political borders of the five concerned countries.

The resulting geological map (Fig. 2, background) illustrates the heterogeneity of the basement, formed during a long geological history. The oldest rocks are of Paleoproterozoic age (gneisses, mylonites and strongly metamorphosed metasediments), attributed to the Rusizian basement. They are largely covered by siliciclastic Mesoproterozoic sediments of the Karagwe-Ankolean Supergroup, in which granitic intrusions were emplaced at about 1370–1380 Ma. Together, they form the Karagwe-Ankole Belt, structured in an Eastern (external) Domain and a Western (internal) Domain, separated by a transition zone with mafic to ultramafic intrusions (Tack et al., 2010; Fernandez-Alonso et al., 2012).

The entire region was subsequently deformed during the Rodinia amalgamation, at about 1000 Ma ago and anorogenic alkaline complexes were emplaced at ~750 Ma (Tack et al., 2010; Fernandez-Alonso et al., 2012). This was followed by the deposition of Neoproterozoic glaciogenic and arenaceous sediments (Itombwe Supergroup) (Cahen et al., 1979; Walemba and Master, 2005) and Karoo sediments in glacial valleys during the Permian (Boutakoff, 1939). The region was again deformed during the late Precambrian – early Paleozoic Pan-African amalgamation of the Gondwana continent. The Neoproterozoic sediments were deformed in a N-S synclinorium (Itombwe syncline), running along the western shore of Lake Kivu and extending further south (Villeneuve, 1976;

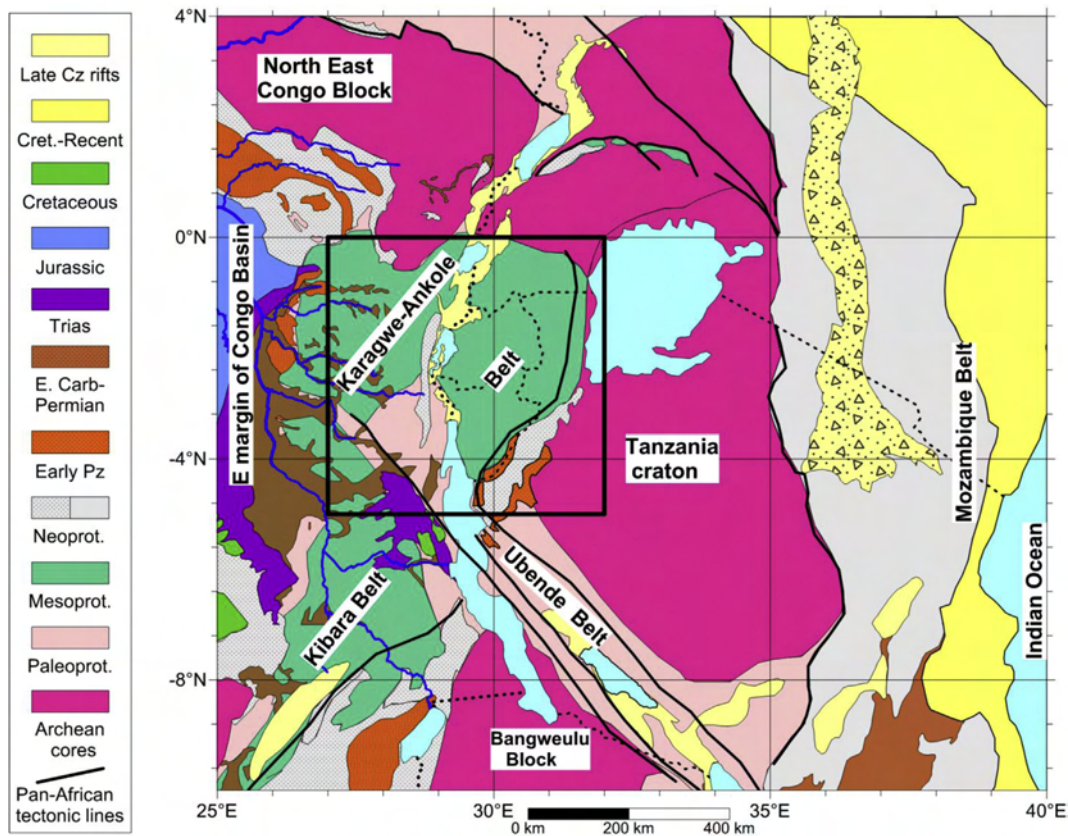


**Fig. 1.** Geological context of the Kivu rift region (area shown as rectangle) within the Mesoproterozoic Karagwe-Ankole belt between the Tanzania Craton, North-East Congo block, Ubende Paleoproterozoic belt and the Congo Basin. It is also located in the middle of the western branch of the East African Rift. It comprises Rwanda and Burundi and parts of Eastern Democratic Republic of Congo, Tanzania and Uganda.

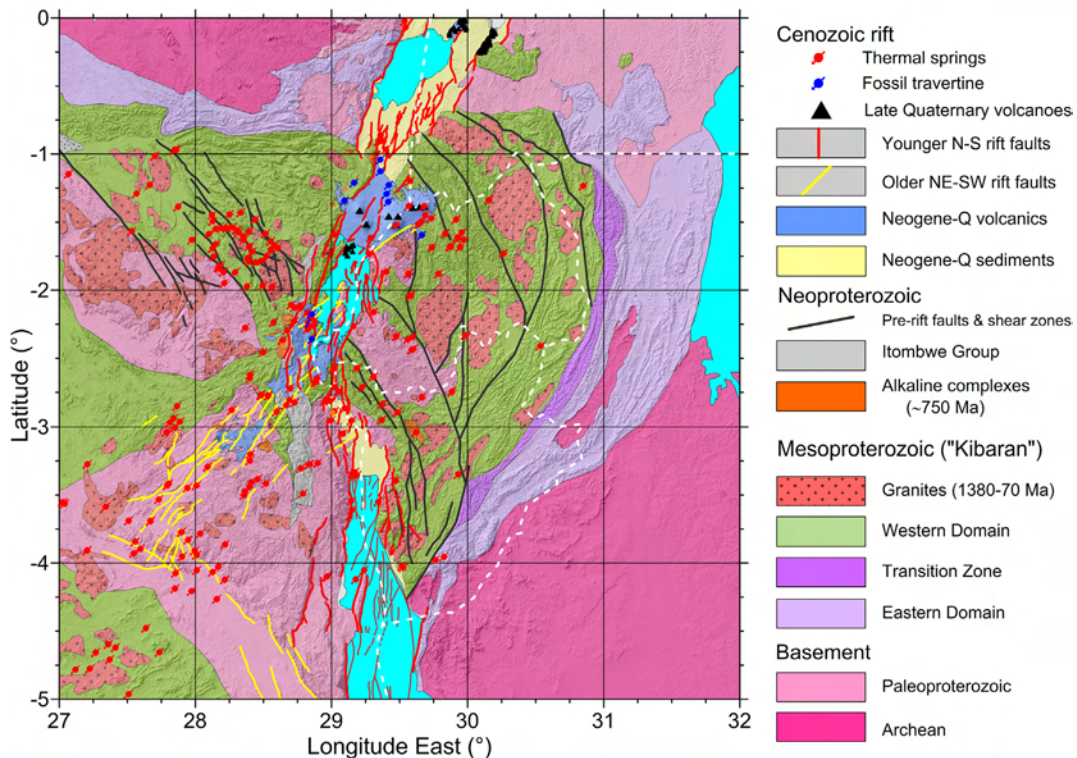


**Fig. 2.** Homogeneous cross-border synthetic geological map of the study region (background) with overprinted neotectonic features (neotectonic faults, late Quaternary volcanic centers, thermal springs and fossil hydrothermal travertine). Hill-shading from the SRTM DEM (90 m resolution).

Lefévére, J., 2003). This deformation occurred in the low grade ductile-brittle domain and generated major faults and shear zones (Brinckmann et al., 2001) that structured the basement before the onset of the late Cenozoic rifting. These lateral heterogeneities in lithospheric structure may have influenced the localization of strain in the Kivu rift area.

## 2.2. Late Cenozoic rifting and active tectonics

Rifting in the North Tanganyika–Kivu region started in the mid-Miocene by extensive volcanism characterized by fissural eruption of continental nephelinites north of the Idjwi Island (20–21 Ma), sodic alkaline basalts along the western side of the Virunga volcanic massif (13–9 Ma) and tholeiitic basalts in the south Kivu rift (11 Ma) (Passau, 1932; Kampunzu et al., 1983, 1998; Tack and De Paepe, 1983; Ebinger, 1989b; Pasteels et al., 1989; Pouclet et al., 2016). These basalts erupted during the doming stage of the rift and during the initial stage of formation of the rift valley, along normal faults sub-parallel to the rift axis. In a later stage, starting around 8–7 Ma, extension localized along a series of major border faults individualizing the subsiding tectonic basins from the uplifting rift shoulders, while lava evolved towards alkali basaltic composition until 2.6 Ma (Ebinger, 1989b; 1991; Wood et al., 2015; Pouclet et al., 2016). In early Quaternary, renewed basaltic volcanism occurred along the south-western margin of Lake Kivu (Villeneuve, 1978; Pouclet et al., 2016). In the late Quaternary-early Holocene, volcanism migrated towards the center of the basin, with the development of the Virunga volcanic massif that dammed the north-directed drainage of the Kivu basin. (e.g. Pasteels et al., 1989; Ross et al., 2014). After a long draught period during the late Glacial Maximum, the lake level rose sharply at ~12 Ka during the Younger Dryas (Ross et al., 2014), concomitantly with the nearby Lakes Tanganyika and Rukwa (Delvaux and Williamson, 2008), until it reached the sill between the Kivu and Tanganyika rift basin, when a new drainage established through the Rusizi valley towards the south, connecting it to Lake Tanganyika (Pouclet, 1978; Ross et al., 2014).

Different maps of rift faults have been proposed based on reconnaissance field surveys (Boutakoff, 1939), interpretation of aerial photographs and satellite images coupled with field work (Degens et al., 1973; Pouclet, 1977, 1978; Villeneuve, 1978, 1980, 1983; Ebinger, 1989b; Laerdal and Talbot, 2002), and on slope-shaded topography and bathymetry (d'Oreye et al., 2011; Wood et al., 2015; Smets et al., 2016).

A deterministic seismic hazard assessment requires a map of active faults for which the past activity of each faults (time of last seismic activation, recurrence rate, maximal magnitude, dimensions, segmentation) is well known. In Sub-Saharan Africa, there are just a few faults where trenching data provide information on earthquake recurrence rates (Vittori et al., 1997; Delvaux et al., 2007; Zielke and Strecker, 2009; Macheyeki et al., 2008). A further complication is the water that fills deep basins, preventing the evaluation of the rupture lengths of many of East Africa's  $M > 6$  earthquakes. Therefore, it is not possible to compile a reliable map of active faults in the Kivu rift region. Instead, we mapped the neotectonic faults, defined as faults which have been active since the onset of the current tectonic regime and stress field and which might still be seismogenic. In our region, the neotectonic faults correspond to those related to the late Cenozoic rifting stage. However, rifting started about 11 Ma ago and evolved in three main stages as reviewed above. Therefore, not every rift fault is currently active, while ancient faults outside the rift zone might still be reactivated under the current stress field.

With these limitations in mind, we compiled a new map of neotectonic faults (those with a marked effect on the

geomorphology), and with a special attention to the chronology of faulting (Fig. 2, foreground). It was performed on the basis of a new interpretation of the Synthetic Radar Terrain Model (SRTM) at 90 and 30 m resolution, complemented by published material and direct field observations. As explained above, the classification and identification of potentially active faults faces the problem of the lack of direct field observations for most of the mapped faults, due to the major difficulties for field access, poor exposure, strong weathering, slope instabilities (landslides) and the presence of the lake. As a consequence, we used indirect indicators to identify faults that are potentially active, such as the presence of morphological fault scarps seen in the SRTM DEM and the occurrence of active thermal springs along them. In the interpretation of the SRTM DEM, we paid also attention to the fault segmentation and branching, avoiding unrealistic combinations of fault segments into single long faults.

For the faults in Lake Kivu and their continuation on-shore (see Fig. 3 for the geographic names), we followed the interpretation of Wood et al. (2015) but in more details on-shore and thus have generally shorter border faults. North of the lake (Virunga volcanic region and Rutshuru basin), we followed more or less closely the interpretation of Smets et al. (2016). Along the western shore of the southern part of the lake, in Katana area, we used the interpretation of Villeneuve (1983), supplemented by our field observation. South of Lake Kivu, the rift zone appears to split into an earlier and currently less active NE-SW branch running from Mwenga to Namoya (Kamituga graben), and the recent and more seismically active Rusizi accommodation zone described by Ebinger (1989b) that connects the Kivu rift basin to the northern termination of the Lake Tanganyika basin in the Rusizi depression (and valley). For this accommodation zone, our interpretation closely follows that of Ebinger (1989b). We mapped the faults of the poorly described Kamituga graben using degraded faceted spurs and fault scarps, using also the compilation of Villeneuve (1977) for the junction area between the two branches.

The Kivu rift region has long been recognised for the occurrence of thermal springs (Boutakoff, 1933; Passau, 1933; Deelstra et al., 1972) and hydrothermal travertine (Verhaeghe, 1963). They often occur along faults and fractures and the thermal waters might reach temperature as high as 90 °C. It is well known that hot springs and associated travertines can be linked to active faults and that the hydrothermal regime can be influenced by earthquakes (Hancock et al., 1999). This relation was also used to identify active faults.

## 2.3. Neotectonic map

The resulting neotectonic map (Fig. 2) shows the mapped faults in relation to the basement geology and the thermal springs. In accordance to Villeneuve (1977) the faults have been classified in two systems: a NE-SW to NNE-SSW (older) population, and a N-S (younger) fault population. The relative chronology between these fault systems has been demonstrated by the same author south of Bukavu. In the Lake Kivu basin, both systems occur together, younger N-trending faults tending to co-exist, crosscut or reactivate older NE- to NNE-trending ones. In the north-eastern part of the lake, Wood et al. (2015) use multi-channel seismic reflection data to show a NE-trending fault that lie in the prolongation of a known fault on land and displace the acoustic basement and older sediments, but not the superficial N-trending faults. South of Bukavu, at the southern extremity of the lake, a young N-trending fault system arranged in an en-echelon way defines the Rusizi depression. It connects further southwards to the major border faults of the northern part of the Tanganyika rift basin, also trending N-S. South of Lake Kivu, the older fault system defines the NE-trending Kamituga graben (Fig. 3) which runs from Walungu to Namoya

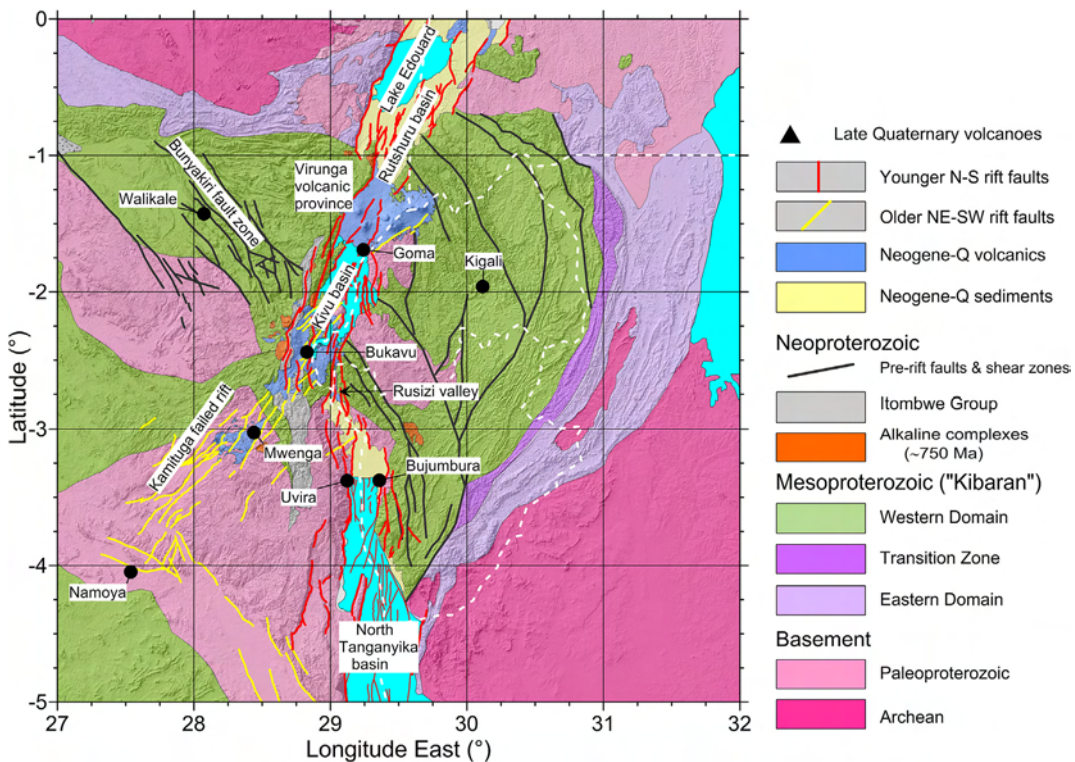


**Fig. 3.** Simplified geological map with the geographic names used in the text. Hill-shading from the SRTM DEM (90 m resolution).

and in which the Kamituga volcanic field (Passau, 1932) developed around 5.8–2.6 Ma ago (Kampunzu et al., 1998). The degraded morphology of the Kamituga graben and border faults suggests that they are currently not as active as the Lake Kivu graben and the Rusizi depression. The Kamituga graben can be interpreted as initiated during the early stage of rifting, together with the rest of the Kivu graben, but abandoned in a later stage when the newly formed Rusizi depression started to accommodate most of the extension. It can therefore be considered as a failed rift, but it is still seismically and hydrothermally active.

Outside the rift valley, a series of faults run in a NW direction from the western shoulder of Lake Kivu, towards the region of Walikale, affecting the Mesoproterozoic series (Bunyakiri fault zone, Fig. 3). They were probably formed as subvertical strike-slip faults during the late Pan-African deformation. These faults present signs of recent tectonic activity as they host numerous thermal springs and coincide with a belt of seismic epicenters. They have been described by Boutakoff (1933) as evidence for the north-western prolongation on the western side of the Kivu rift, of the NW-SE rifting direction typical of the Central Tanganyika and Rukwa rift. Here, we re-interpret them as a reactivation of pre-existing faults formed during the pre-rift history. On the western side of the map, the strike-slip earthquake of Mw 5.5 on 30/11/2013 activated one of the faults at that limit the Paleoproterozoic basement from the Mesoproterozoic metasediments (Harvard Centroid Moment Tensor catalogue).

### 3. Seismotectonic setting

Besides seismicity, the seismic hazard of a region depends also on its seismotectonic features such as the dimension of faults, faulting depth and the stress regime (McCalpin, 1996; Scholz, 2003).

#### 3.1. Empirical estimation of maximum magnitude

We made a first empirical estimate of the regional maximum magnitude (maximum credible earthquake) on the basis of the empirical relationship between rupture length and earthquake moment magnitude of Wells and Coppersmith (1994):

$$M_{\max\_rl} = 5.08 + 1.16 \log (\text{Rupture Length})$$

with Rupture Length as the measured length of the surface rupture, in km. Using the neotectonic faults compiled above, we obtained a distribution of magnitudes  $M_{\max\_rl}$  between 5.4 and 7.3, assuming that their entire length will rupture during the fault activation (Fig. 4). The longest faults giving magnitudes of 7 or above are all located on the margin of the rift basins, acting as border faults. As in the Ethiopian rift, such faults are the longest in the fault population (e.g. Hayward and Ebinger, 1996) and have been probably the first to develop during the initiation of rifting. We also know that during rifting, deformation tends to migrate towards the central part of the basin, along a large number of smaller faults (Corti, 2012; Keir et al., 2015), and that in an advanced stage of rifting, the large border faults are progressively abandoned. We are aware that many more recent magnitude-length scaling relationships exist (e.g. Wesnousky, 2008; review in Stirling and Goded, 2012) but will not use these results in the seismic hazard assessment because of too high uncertainties associated with our data.

#### 3.2. Depth of faulting and mechanical properties of the crust

Most earthquake hypocenters determined by local seismic networks are located in the intermediate to shallow crust. Wohlenberg (1968) reported hypocentral depths ranging between 5 and 19 km for the Kivu Lake basin, the Rusizi valley and its junction with the North Tanganyika basin. Deeper events are also

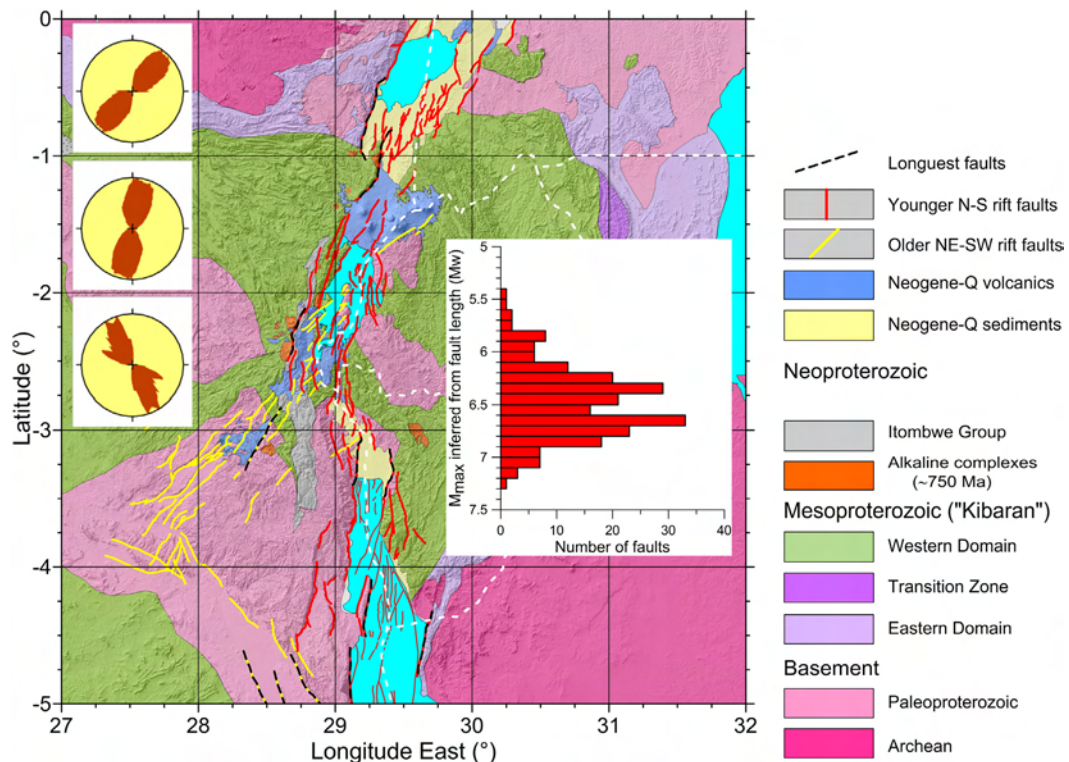


**Fig. 4.** Estimated maximum magnitude  $M_{\max}$  based on the relation between fault length and the empirical relation of Wells and Coppersmith (1994). Simplified geological map with the two systems of rift faults: older NE-SW and NW-SE (SW corner of the map) and younger N-S. Rose diagrams of corresponding fault orientation (equal area, moving average with  $15^{\circ}$  aperture). Histogram of estimated  $M_{\max}$ . Hill-shading from the SRTM DEM (90 m resolution).

reported outside the rift basin by Wohlenberg (1968), but there are unreliable as they fall outside the IRSAC seismic network. Zana and Hamaguchi (1978) reported depth ranging between 5 and 15 km for the aftershock sequence of the 1960-09-22 Uvira earthquake, measured within the IRSAC network. For the Virunga area, both Tanaka (1983) and Wood et al. (2015) found relatively shallow events beneath the active volcanoes (8–14 km), with more diffuse seismicity down to 20 km. In the central part of the Kivu basin, earthquakes determined by Wood et al. (2015) are all less than 15 km deep. The 2008 Bukavu-Cyangugu earthquake was modelled at 9 km deep using a combination of teleseismic and InSAR data (d'Oreye et al., 2011).

To precise the average hypocenter depth for the Kivu region, we considered only the events determined from waveform inversion and modelling. A total of 31 events have been compiled from Barth et al. (2007), Craig et al. (2011), d'Oreye et al. (2011) and from the Harvard Centroid Moment Tensor database (Appendix A, Fig. 5). They cover most of the rift structure, and also the western rift flank, including the Kamituga failed rift branch. The epicentral depth ranges mainly between 7 and 15 km, with a few deeper (but not always well-constrained) events and a shallow event (3 km). In the seismic hazard modelling, we will use the average depth of 11 km for the 27 events which are not deeper than 15 km.

Examined at the scale of the entire western rift branch, the Kivu rift segment has a shallower seismicity and lower observed maximum magnitude than the rest of the western rift branch (Yang and Chen, 2010; Craig et al., 2011). The maximum observed earthquake of the Albertine - Rwenzori segment is the Mw 6.9 1966 Uganda-Toro earthquake (Craig et al., 2011) and of the South-Tanganyika - Rukwa segment is the Ms 7.4 1910 Rukwa earthquake (Ambraseys, 1991) while the Ms 6.3 1960 Uvira earthquake (Zana and Hamaguchi, 1978) is the strongest for the Kivu rift

segment. A low velocity zone at 100 km deep below the Kivu rift region has been identified by Adams et al. (2012), suggesting a strong thermal perturbation at depth that causes a reduction in plate strength and which might have an influence on the mechanical behaviour at shallow depth. This anomaly might be responsible for the presence of a warmer crust with shallower crustal earthquakes (<15 km) in the magmatic Kivu region, while the other parts western rift branch are in a colder crust with deeper crustal earthquakes (down to 35 km). Moreover, magma intrusion related to the volcanic activity might also have an effect on thermal gradients, and consequently, on mechanical properties. But, at the scale of the Western Rift, this process seems not so important, as shown by the high proportion of geodetic moment seismically accommodated (Déprez et al., 2013).

### 3.3. Stress pattern and ability of faults to slip

Focal mechanisms are also available for the same data set of earthquakes determined from waveform modelling. Most of the events are of normal faulting type, except two on the western rift shoulders which are of strike-slip type (Fig. 6). The direction of horizontal principal extension ( $S_{h\min}$ ) is in general sub-orthogonal to the trend of the rift segments, with sometimes a slight obliquity. On the western rift shoulder, the direction of extension tends to rotate quickly into a N-S direction, matching the stress field which characterises the margin of the Congo Basin (Delvaux and Barth, 2010). On the southwestern part of the map (Elila region), the extension direction is more NW-SE, sub-orthogonal to the Kamituga failed rift. The stress field appears to be laterally variable, requiring more constraints on crust and mantle lithospheric structure.

The ability of a fault to slip in a given stress field depends on the

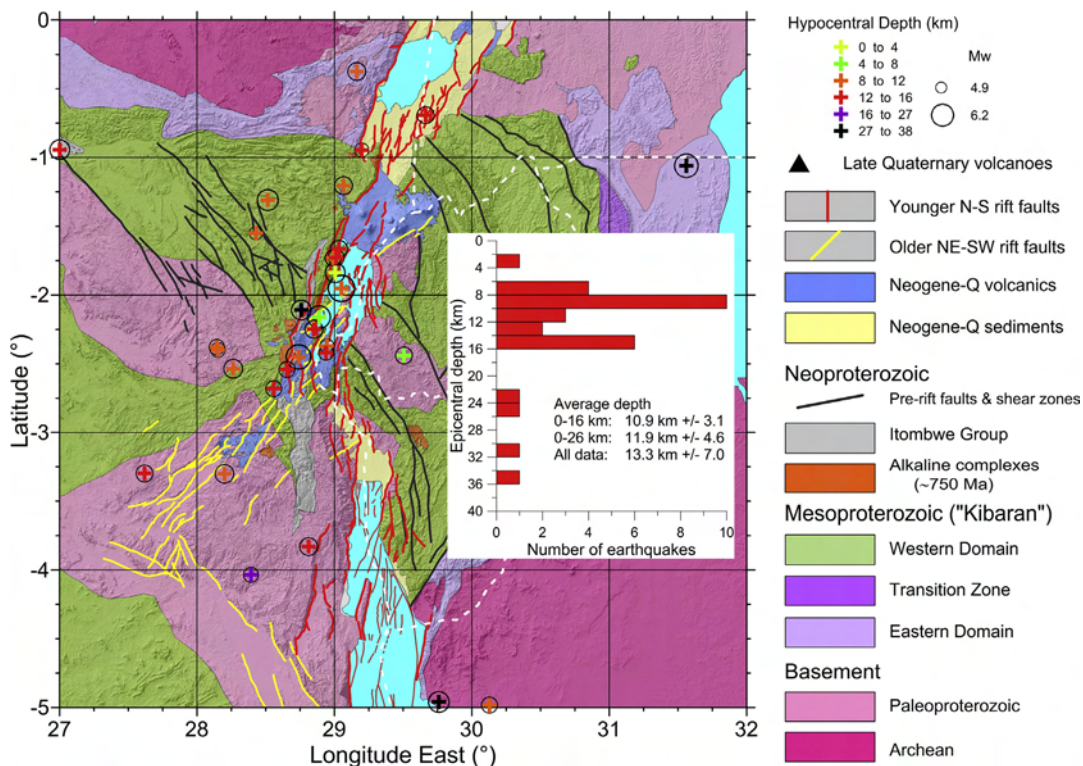


**Fig. 5.** Earthquake hypocentral depth from events determined with waveform modelling (data from Appendix A, colors of crosses indicating hypocentral depth and circle proportional to magnitude). Histogram of hypocentral depth. The deep hypocenters (>20 km) are probably due to errors in hypocenter location. Hill-shading from the SRTM DEM (90 m resolution). (For interpretation of the references to colour in this figure legend, the reader is referred to the web version of this article.)

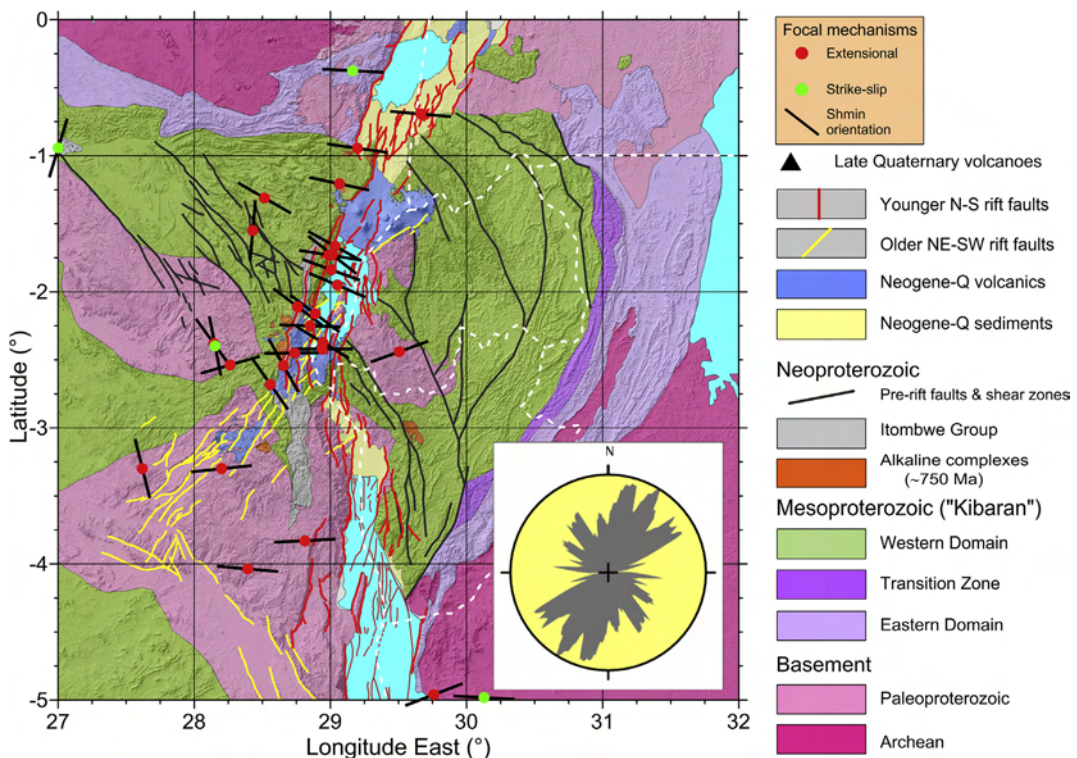


**Fig. 6.** Tectonic stress from Earthquake focal mechanisms from events determined with waveform modelling (data from Appendix A, colour in function of the tectonic regime and bar oriented in function of the horizontal minimum stress direction Shmin). Rose diagram of focal planes orientation (movement and auxiliary planes). Hill-shading from the SRTM DEM (90 m resolution). (For interpretation of the references to colour in this figure legend, the reader is referred to the web version of this article.)

ratio of the shear and normal stress acting on the plane and its frictional characteristics (Morris et al., 1996). This implies, at constant frictional conditions, that the faults which are more favourably oriented relative to the stress field will be preferentially reactivated. In a region affected by an Andersonian extensional stress field regime as here, normal faults oriented at a high angle to the horizontal principal extension and inclined at about 60° from the horizontal will be favoured. The stress pattern over the Kivu region clearly suggests that the recent N-S faults of the active rift valley are in favourable orientation for being reactivated (sub-orthogonal to the  $S_{\text{hmin}}$  directions). The lateral variation of the stress trajectory on the western shoulder of the rift also suggests that the NE-trending normal faults of the Kamituga failed rift can also be reactivated, as the NW-trending (subvertical?) faults of the Bunyakiri fault zone in Masisi region.

#### 4. Earthquake catalogue

A new catalogue of macroseismic and instrumental seismicity for the period ranging from 1888 to 2015 (127 years) was compiled with 1031 events of magnitude Mw or equivalent ranging from 1.4 to 6.3 for the region between 27 and 32° E and 0–5° S. We added 37 macroseismic events to the catalogue by assessing reports of felt seisms. For the seismic hazard assessment, the modelling requires a catalogue without duplications and dependent shocks, and with homogeneous magnitudes (e.g. Joshi and Sharma, 2008; Kijko, 2008). This requires the classical operations of duplication removal, magnitude homogenisation and aftershocks removal.

##### 4.1. Instrumental catalogue

Instrumental data were compiled from the Reviewed ISC Bulletin from the International Seismological Center in UK, for 1970 to end 2015 (not reviewed for the last six months). In this bulletin, we choose, the events (timing and location) and their magnitude determined by the following seismic agencies by order of priority (acronyms of seismic agencies defined in Appendix B): the ISC, BUL (until 1990), EAF (since 1991), ENT, NAI, PRE and LSZ. We completed it with events from the CGS (Council for Geosciences) catalogue, NEIC (National Earthquake Information Center) and GSHAP (Global Seismic Hazard Assessment Project; Turyomurugendo, 1996) which were not yet present in the ISC catalogue. For the largest magnitudes, we used the last published Mw magnitudes obtained by waveform modelling (Kebede and Kulhanek, 1991; Barth et al., 2007; Yang and Chen, 2010; Craig et al., 2011; d'Oreye et al., 2011; Biggs et al., 2013; Harvard Centroid Moment catalogue).

Historical and/or early instrumental data were taken from Ambraseys (1991) and Ambraseys and Adams (1986, 1991). We used also data from the IRSAC seismic network (LWI) which was progressively set up between 1953 and 1955 (De Bremaeker, 1956) and became fully operational between 1956 and 1963 (Wolhengberg, 1969). From this catalogue, we kept only the events determined by at least three stations and the same is done for the other catalogues when the number of stations is given (ISC and CGS).

##### 4.2. Additional historical seismicity from felt seismic events

The instrumental catalogue covers a relatively short period of observation, as the earliest fully instrumental seismicity dates back only to 1945 in the region. In an attempt to extend the duration of the catalogue, we determined new historical seismic events from records of felt seismic shocks. As early as at the beginning of the colonial times, explorers and geologists occasionally reported felt seismic shocks the eastern part of the DRC and adjacent regions of

Uganda, Rwanda and Burundi (Cornet, 1910; Passau, 1911, 1912; Krenkel, 1922; Sieberg, 1932). The Belgian administration asked all operators of meteorological stations to record also the felt seismic events (Gasthuys, 1939). Those stations became particularly numerous in Rwanda and Burundi. In parallel, the Geological Survey of Uganda installed a seismic station in Entebbe and reported seisms felt in western Uganda (Wayland and Simmons, 1920; Groves, 1929; Simmons, 1929, 1939; Willis, 1936).

In 1958, Herrinck (1959) compiled a list 960 felt earthquakes recorded at the meteorological stations between 1915 and 1954 in Congo, Rwanda and Burundi. We completed this database by exploiting the meteorological archives and available historical reports to enlarge the database to 1513 entries between 1900 and 1959, including those from Uganda. These entries have been examined in order to identify possible historical seismic events (Mulumba and Delvaux, 2012). Possible events are identified by three or more quasi-simultaneous records observed at stations located over a relatively short distance from each other (max. 1–2 degrees of latitude/longitude) and within a short time difference (few hours). A total of 37 possible historical earthquakes have been obtained for the Kivu region, for which four or more shocks (including close aftershocks) have been felt at two or more different stations (Appendix C). The proposed location is taken as the average latitude and longitude of the stations where the felt seismic was recorded.

The magnitude of each event is estimated from an empirical relation between magnitude and perception distance determined from the data of Ambraseys (1991) on the Rukwa 1910 seismic sequence. This remains, however, dependent on the possible spatial incompleteness of the record of felt seismic evidence. For three of the more recent events, locations and magnitudes are also available from the ISC catalogue. The magnitude estimation is almost similar but the location differs by up to 2°. In particular, the event of 1945-03-04 which was determined by Gutenberg and Richter (1954) on the basis of macroseismic evidence in Uganda was relocated south-westwards in Rwanda because our database shows that it was also felt in the DRC and Rwanda.

##### 4.3. Catalogue merging and magnitude homogenisation

Both instrumental and historical seismic data were merged into a single catalogue (Supplementary Material 1), the duplicates removed and the magnitudes homogenized to Mw. In the removal of duplicates, we kept by order of preference, the events for which the solution was obtained by waveform modelling (Appendix A), then the solutions from the ISC catalogue, with the exception mentioned just above. The original catalogues contain a total of 1068 events since 1888, of which 1154 for 1931–2015 (85 years). From 1888 to 1930, only a few poorly determined historical events

**Table 1a**

Statistics for the new seismic catalogue and sub-catalogues for the Kivu region with time range, completeness characterisation and number of data for original data compilation (duplicates removed), independent or declustered data (indep.) and data with magnitude equal or above the magnitude of completeness Mc.

Catalogues	Completeness			Number of data		
	Years	Mw Obs	Mc	Original	Indep.	$\geq$ Mc
	1888–1930			4		
Cat 1	1931–1955	4.2–6.16	4.4	44	42	39
Cat 2	1956–1965	1.4–6.32	3.7	476	366	327
Cat 3	1966–1989	4.2–5.7	4.6	238	210	172
Cat 4	1990–2015	2.0–6.2	4.1	305	230	179
All cat.				1068	848	717
Cat 2–4	1956–2015		4.4	1020	806	359

are known, so this period is no further considered. The contribution of the different agencies to the catalogue, event location and magnitude determination is detailed in [Table 1a](#).

In order to homogenize the magnitudes, equivalent Moment magnitudes Mw-eq have been obtained using the empirical relations of [Scordilis \(2006\)](#) linking Ms to Mw:

$$\text{Mw-eq} = 0.67 (\pm 0.05) \text{ MS} + 2.07 (\pm 0.03) \text{ for } 3.0 \leq \text{MS} \leq 6.1$$

$$\text{Mw-eq} = 0.99 (\pm 0.02) \text{ MS} + 0.08 (\pm 0.13) \text{ for } 6.2 \leq \text{MS} \leq 8.2$$

or from Mb:

$$\text{Mw-eq} = 0.85 (\pm 0.04) \text{ Mb} + 1.03 (\pm 0.23) \text{ for } 3.5 \leq \text{Mb} \leq 6.2$$

When both Mb<sub>(ISC)</sub> and MS<sub>(ISC)</sub> are available, we used the conversion from MS as the body-wave Mb magnitudes saturate at magnitudes levels below that of the surface-wave magnitudes MS ([McCalpin, 1996](#)).

For the catalogue provided by [Wohlenberg \(1968\)](#) for the IRSAC (LWI) network, [Mavonga and Durrheim \(2009\)](#) have shown that, for magnitudes greater than 4, the M<sub>(LWI)</sub> magnitudes are systematically too high, while for magnitudes less than 4.0, they are consistent with the Richter local magnitudes. For the higher magnitudes, we used the successive corrections proposed by the same authors:

$$\text{Mb}_{(\text{USGS})} = 0.282 \text{ M}_{(\text{LWI})} + 3.315$$

$$\text{Mb}_{(\text{ISC})} = 0.90 \pm 0.14 \text{ Mb}_{(\text{USGS})} + 0.38 \pm 0.06$$

Similarly the magnitudes Mb<sub>(BUL)</sub> have been corrected using the relation of [Mavonga and Durrheim \(2009\)](#):

$$\text{Mb}_{(\text{ISC})} = 0.59 \pm 0.08 \text{ Mb}_{(\text{BUL})} + 1.97 \pm 0.26$$

We are aware that concerns exist on the magnitude determination by BUL. Most of the data with magnitudes provided by BUL come from the ISC reviewed catalogue and all prior to February 1993, before the magnitude determination became unreliable ([Midzi, pers. Comm.](#)).

For data provided by ENT, the magnitude ML was taken as equivalent to Mb<sub>(ISC)</sub> without correction. In these 3 cases, the Mb<sub>(ISC)</sub> magnitudes have been further converted into Mw-eq using the Scordilis relation above. When performing these corrections, we noticed that the original M<sub>(LWI)</sub> magnitude are converted to higher final Mw magnitude for M<sub>(LWI)</sub> lower than 4.8. Therefore, we corrected the M<sub>(LWI)</sub> magnitudes only for those equal to or above 4.8.

#### 4.4. Catalogue heterogeneity

A plot of the magnitude versus time ([Fig. 7a](#)) shows that the resulting catalogue is highly heterogeneous. It can be subdivided into 4 sub-catalogues with different range of observed magnitudes ([Table 1b](#)). On the neotectonic map ([Fig. 7b](#)), the seismicity of the Kivu rift region appears relatively scattered with some first-order concentration in the North Tanganyika graben, the Kivu basin, and the Rutshuru basin, as well as on the western shoulder of the Virunga volcanic province. Second-order concentration along fault zones cannot be observed, possibly due to the relatively large error in epicentral location for most of the events in the catalogue.

#### 4.5. Removal of dependent events

The next operation is to remove the dependent events (aftershocks and volcano-tectonic), related either to sismo-tectonic

events or to volcanic eruptions. Several aftershock sequences of major earthquakes and volcanic eruptions have been described in the Kivu region:

- Uvira seism (1960-09-05, Ms 6.3) ([Zana and Hamaguchi, 1978](#));
- Uvira seism (1962-03-08, Ms 5.5) ([Ambraseys and Adams, 1986](#));
- Uganda-Toro seism (1966-03-20, Mw 6.9), with the main shock north of our studied region but with some aftershocks with the limits of the studied region ([Wohlenberg, 1968; Craig et al., 2011](#));
- Masisi seism (1995-04-29, Mb 5.1) ([Mavonga, 2007](#));
- Nyiragongo volcanic eruption (2002-01-17), with a long series of associated volcano-tectonic and volcanic earthquakes with the largest at Mb 4.8 during the following months, up to 2002-05-17 ([Mavonga, 2007; Tedesco et al., 2007; Shuler and Ekström, 2009; Wauthier et al., 2012](#));
- Kalehe seism (2002-10-24, Mw 6.2) which occurred 9 months after the 2002 volcanic eruption of the Nyiragongo volcano, at the limit of the zone affected by the volcano-tectonic aftershocks, possibly triggered by Coulomb stress perturbation related to the dyking event of the volcanic eruption ([Wauthier et al., 2015](#));
- Bukavu seism (2008-02-03, Mw 6.0) ([d'Oreye et al., 2011](#));
- Katana seism (2015-08-07, Mw 5.8; aftershocks until at least February 2016).

Earthquake aftershock distribution follow empirical relations ([Shcherbakov et al., 2004](#)), the G-R frequency-magnitude scaling, the Omori law for the temporal decay of aftershock rates ([Utsu, 1961](#)) and the Båth law following which the maximum magnitude of aftershocks is between 1.0 and 1.2 less than the main shock ([Båth, 1965](#)).

Here, the dependent events were removed by considering that aftershocks occur within a radius distance and a number of days depending on the magnitude of the main shock as follows:

- 1.2° (132 km) radius and 120 days for Mw ≥ 6.0
- 0.75° (99 km) radius and 60 days for Mw ≥ 5.5
- 0.5° (66 km) radius and 30 days for Mw ≥ 5.0

We found that they occur with a maximum magnitude lower than that of the main shock by 1.35 units in average, but which can be as low as 0.3 units. We removed also the series of volcano-tectonic earthquakes associated to the Nyiragongo volcano 2002 eruption (references given above). We removed a total of 220 dependent events and got a final number of 848 independent events for the period ranging from 1931 to 2015.

#### 4.6. Catalogue completeness

Using the independent events, the magnitude of completeness for the different catalogues has been estimated visually from the Gutenberg-Richter plots, from the break in slope towards the lower magnitudes ([Fig. 8; Table 1b](#)).

Between 1931 and 1955, from the 42 independent remaining events, 39 are above  $M_c = 4.4$ , but most of them are macroseismic events. Due to the rough estimate of their location and magnitude, they will not be used in seismic hazard assessment. The period 1956–1965 corresponds to the activity of the IRSAC seismic network established around Lake Kivu, with observed equivalent magnitudes Mw-eq ranging between 1.4 and 6.3 and a magnitude of completeness  $M_c = 3.7$  (327 independent events above  $M_c$ ). After 1965, the IRSAC network was no longer operational and the instrumental seismicity was recorded by the regional seismic

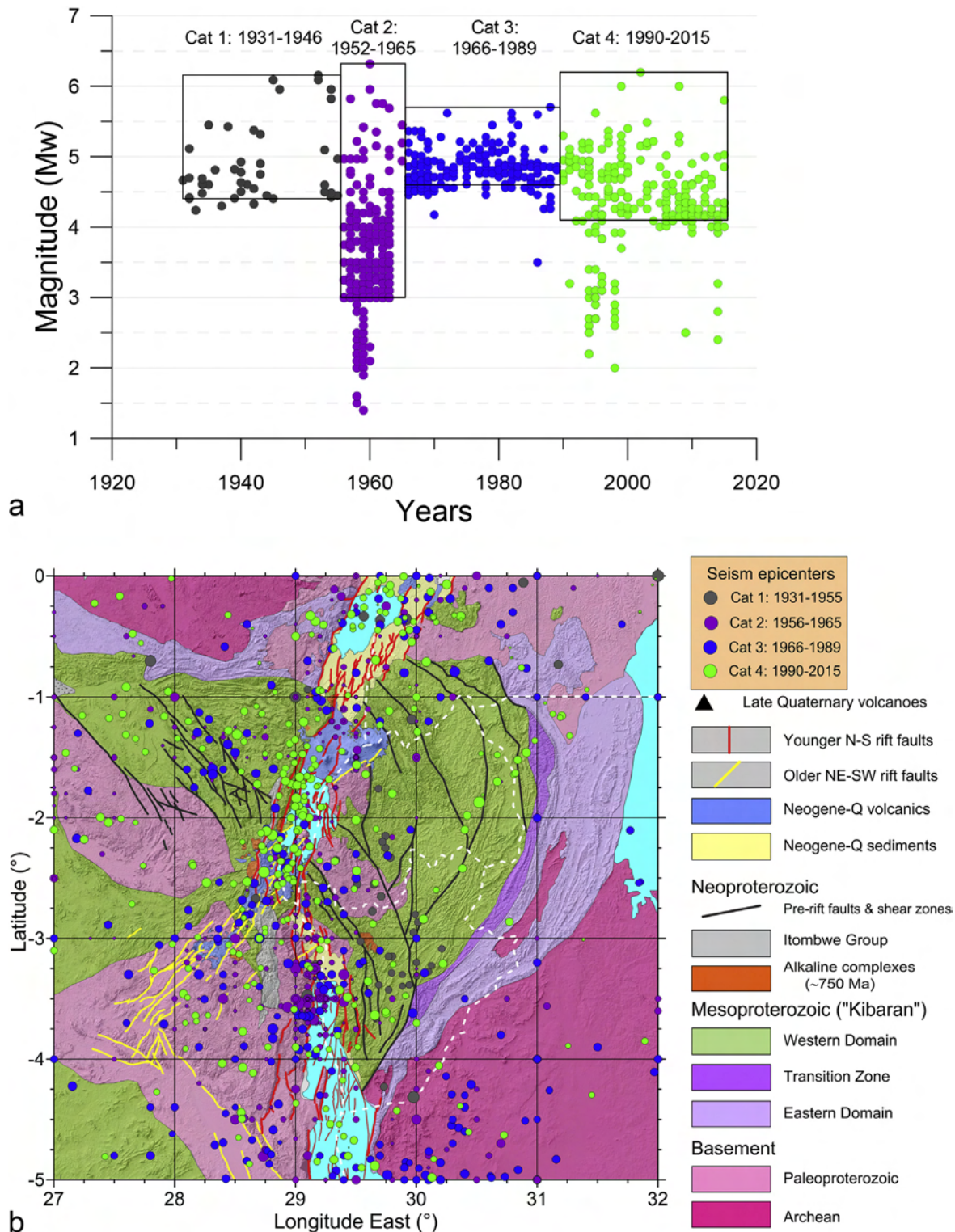


**Fig. 7.** Characteristics of the new seismic catalogue compiled for the Kivu rift region (duplicates removed, but not declustered). a: Time-magnitude distribution of events from the catalogue of seismicity with separation into 4 sub-catalogues. b: distribution of seismic epicenters with colors in function of the sub-catalogues and points scaled un function of equivalent Mw magnitude (0.8–6.3). Time range: 1931–2015 (1154 data).

networks that were progressively setup in the neighbouring regions. The level of magnitude detection dropped to  $M_{\text{w-eq}} \geq 4.2$  up to 1989, with  $M_c = 4.6$  (172 independent events above  $M_c$ ). During the last period (1990–2015), events as low as  $M_{\text{w-eq}} = 2.00$  have been recorded, but with a  $M_c = 4.1$  (179 independent events above

$M_c$ ). Most of the events with magnitude  $M_{\text{w-eq}}$  below 4.0 that appear after 1995 are from the ISC catalogue, from the EAF and ENT agencies. They reflect the extension of the regional seismic networks during this period.

As it appeared difficult to work with three different sub-

**Table 1b**

Data provenance in function of the origin catalogue, location determination and magnitude determination (Acronyms of seismic agencies defined in Appendix B).

Catalogue		Location		Magnitude	
Agency	Data	Agency	Data	Agency	Data
RMCA	35	RMCA	35	RMCA	38
IRSAC	448	WOHL	448	LWI	459
ISC	515	ISC	313	ISC	138
CGS	47	CGS	40	CGS	0
GSHAP	7	GSHAP	7	GSHAP	21
HAR	2	HAR	3	HAR	7
NEIC	5	NEIC	8	NEIC	10
Publications	9	Publications	18	Publications	19
Total	1068	BUL	76	BUL	238
		EAF	48	EAF	72
		ENT	10	ENT	11
		IDC	39	IDC	39
		PRE	2	PRE	3
		NAI	5	NAI	9
		LSZ	2	LSZ	3
		USGS	1	NOAA	1
		Others	13		

catalogues of different levels of completeness, we extracted a unique catalogue by merging the three catalogues from 1956 to 2015 and extracted 359 independent events with  $M_{\text{W-eq}} \geq 4.4$  and used this new catalogue in the seismic hazard assessment. The common minimum  $M_c$  magnitude for each of the separate sub-catalogues used is 4.6, but we used 4.4 instead to allow a finer definition of  $M_c$  for each zone. As we will see later, the effective  $M_c$  in all zones but one was found at 4.6. In this final catalogue, on which the seismic zoning and hazard analysis was done (Supplementary material 2), only 18 events from the IRSAC catalogue remain.

## 5. Seismic source zones definition and characterisation

The definition of seismic sources on the basis of known active faults is not possible in the present case, because of the lack of detailed characterisation of active faults in this region. As an alternative, we defined seismic source zones over which the Gutenberg-Richter (G-R) parameters that are necessary for the seismic hazard assessment are considered uniform. Those are  $M_c$ , the magnitude of completeness of the catalogue;  $M_{\text{max}}$ , the maximum regional magnitude;  $\lambda$ , the mean seismic activity rate and the a-value (intercept of the G-R linear fit), and b-value (power-law of the magnitude distribution and slope of the G-R fit, indicating the relative weight of large versus small events). The G-R parameters are determined assuming that earthquake magnitudes follow a double-truncated G-R cumulative magnitude-frequency distribution with a Poissonian model of earthquake occurrence and that the catalogue is complete above the magnitude threshold  $M_c$  (e.g. Sornette and Sornette, 1999; Joshi and Sharma, 2008; Kijko, 2008):

$$\text{Log}(N) = a - b * M_{\text{W-eq}}$$

with  $M_{\text{W-eq}}$ : the equivalent moment magnitude since the magnitudes other than Mw have been converted into Mw, a and b: the parameters describing the linear fit to the magnitude-frequency distribution and N: the number of events per year having magnitudes  $\geq M_{\text{W-eq}}$ .

### 5.1. Seismic zonation

The definition of the seismic source zones was done on the basis

of the new geological and neotectonic maps as compiled above (Fig. 2), taking into account the basement structure and the distribution of neotectonic faults, thermal springs and Quaternary volcanic centers. It was not done on the basis of the seismicity alone because of the catalogue incompleteness, inhomogeneity and sometimes poor accuracy in epicenter location. The Kivu rift region was split into 7 seismic zones (coordinates in Supplementary material 3) with a number of data per zone varying from 33 to 76 (Fig. 9, Table 2). In principle 50 events are enough to assess the value of  $M_{\text{max}}$  when magnitudes follow the Gutenberg-Richter relation with b-value close to 1 (Kijko, 2004).

The rift valley itself has been split into several seismic zones: the Virunga - Rutshuru (1), Lake Kivu (2), and Rusizi - North Tanganyika (3) zones. They represent different sectors of the rift valley, marked by specific seismic activity. The Virunga - Rutshuru zone (1) comprises the entire volcanically active sector of the Kivu rift, extending from the Toro-Ankole and Bunyarunguru volcanic fields, respectively north and northeast of Lake Edward in the Rusthuru rift basin, to the active Nyiragongo and Nyamulagira volcanoes in the Virunga volcanic fields, and extending to the underwater late Quaternary volcanic cones evidenced by Ross et al. (2014) on the northeastern extremity of Lake Kivu. The strongest event recorded in this zone ( $M_{\text{W-eq}} 5.4$ , 1968-06-29) is from the ISC catalogue.

The Lake Kivu zone (2) is structured as a first-order west-dipping half-graben (Wood et al., 2015) with a major border fault scarp on its western side and two directions of smaller internal faults as discussed above. It extends from the Kalehe horst, just south of the underwater late Quaternary volcanic cones, and up to Mwenga, about 50 km south of the city of Bukavu along the southern extremity of the lake. It also contains evidence of recent volcanism along the western margin of the basin, but of early Quaternary age (Villeneuve, 1978; Kampunzu et al., 1983; Pasteels et al., 1989; Pouclet et al., 2016). It was affected by the 1912-03-08  $M_{\text{W-eq}} 6.1$  Lake Kivu, 2002-10-24, Mw 6.2 Kalehe, 2008-02-03 Mw 6.0 Bukavu-Cyangugu (d'Oreye et al., 2011) and, recently, the 2015-08-07 Mw 5.8 Katana earthquakes.

The Rusizi - North Tanganyika zone (3) represents the accommodation zone between the Lake Kivu and the North Tanganyika rift basins (Ebinger, 1989b), controlled by en-echelon N-S normal faults. Lava flows of 5–6 Ma old have been recognised in the Rusizi plain in Burundi (Tack and De Paepe, 1983; Pasteels et al., 1989). This zone was affected by the 1952-01-31  $M_{\text{W-eq}} 6.2$  in Burundi (De Bremeker, 1956), and the 1960-09-22, Uvira earthquakes with three main shocks, at 5hr38 ( $M_{\text{W-eq}} 6.0$ ), 9hr05 ( $M_{\text{W-eq}} 6.3$ ) and 9hr14 ( $M_{\text{W-eq}} 6.2$ ) (Wohlenberg, 1968, 1969; magnitudes revised by Turyomurugyendo, 1996). The 1952 event is not considered in the present seismic hazard assessment as we consider only the period starting in 1956. The three events of 1960 are from the ISC catalogue, and the  $M_{\text{W-eq}} 6.3$  is still the strongest earthquake recorded in the Kivu rift region.

On the southwestern part of the map, the Elila zone (4) corresponds dominantly to Paleoproterozoic metasediments, affected by the early stage of the late Cenozoic rifting. As mentioned above, the NW-trending normal fault system that lies in the prolongation of the Kivu basin defines the Kamituga failed rift depression. The Elila zone comprises also the high plateau that forms the western shoulder of Lake Tanganyika (Mitumba Mountains). The strongest event in this zone ( $M_{\text{W-eq}} 5.8$ ) is from the ISC catalogue, determined by GSHAP.

On the western side of the rift valley, the Masisi zone (5) corresponds to Mesoproterozoic metasediments with large granitic intrusions affected by the Bunyakiri NW-trending fault system of probable late Pan-African age. It appears still active as shown by significant seismicity and thermal springs concentrated along this fault zone (Boutakoff, 1933). The strongest earthquake occurred

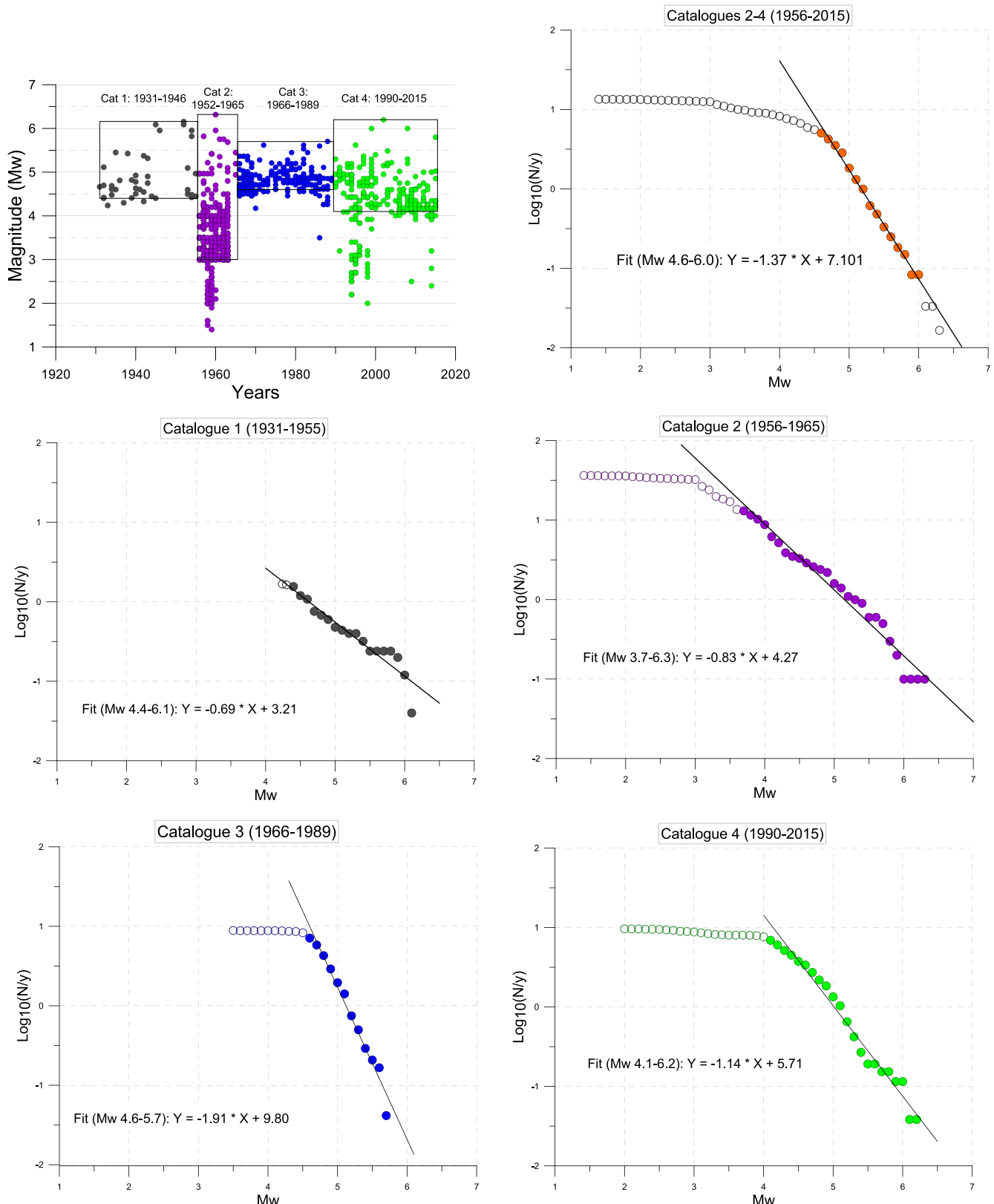


**Fig. 8.** Gutenberg and Richter analysis (cumulative number of earthquake per year versus magnitude) by double-truncated least square linear fit to the observed data for the four sub-catalogues and the combined sub-catalogues 2, 3 and 4. The data used are displayed as plain circles. The lower magnitude correspond to the estimated magnitude of completeness  $M_c$ . For the combined catalogue, the upper magnitude was set in order to remove the effect of the largest magnitudes. Declustered catalogues, without a priori removal of magnitudes lower than  $M_c$ . The number of data per sub-catalogue is given in Table 1, the computed Gutenberg and Richter relations are indicated on the graphs and the parameters displayed in Table 3 (upper part).

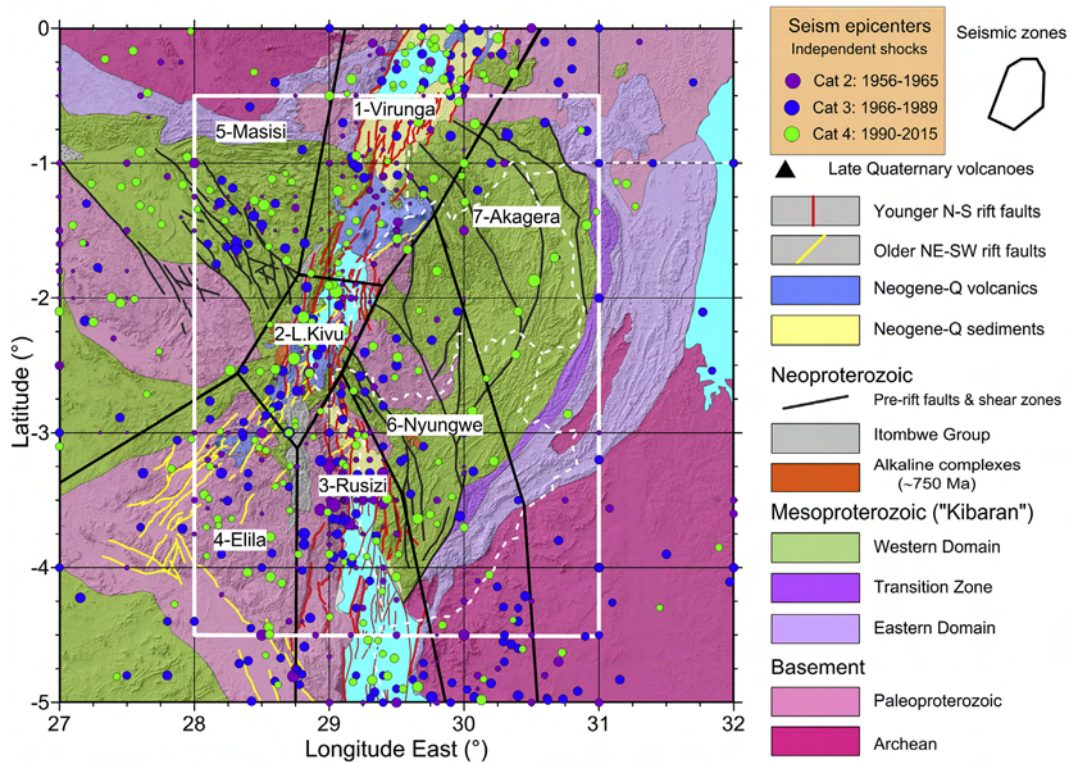


**Fig. 9.** Study region with outlines of the seven seismotectonic source zones defined for seismic hazard calculation (marked by black polygons, numbered), together with seismicity and fault map. Plotted on top of general geological map, with hill-shading from the SRTM DEM (30 m resolution).

close to this fault zone on 1995-04-29, with  $Mw = 5.4$  (Barth et al., 2007).

East of the rift valley, the Nyungwe zone (6) corresponds to the

highlands forming the eastern shoulder of the Kivu rift. Only moderate seismicity has been recorded since instrumental recording commenced in 1954, although a series of seismic shocks

**Table 2**

Maximum magnitude  $M_{max}$  values determined by the maximum likelihood method using the program AUE of Kijko and Smit (2012). Upper part: for the sub-catalogues, lower part: for the seismotectonic source zones and for the entire region (all zones). Data: number of data by zone,  $Mc$ : Magnitude of completeness,  $M_{max-obs}$ : maximum observed magnitude,  $M_{max-obs} + 0.3$ : maximum observed magnitude incremented by 0.3.  $M_{max}$  values and their variance obtained with the methods of Gibowicz-Kijko (G-K: Gibowicz and Kijko, 1994), Gibowicz-Kijko-Bayes (G-K-B: Kijko and Singh, 2011), Kijko-Sellevoll, (K-S: Kijko and Sellevoll, 1989), Kijko-Sellevoll-Bayes (K-S-B: Kijko, 2004) and non-parametric Gaussian (N-P-G: Kijko, 2004). The average value of  $M_{max}$  and the variance are presented for the values obtained with a variance lower than 0.40.  $M_{max\ ave - obs}$ : difference (increment) between  $M_{max-obs}$  and the average  $M_{max\ ave}$ . With a grey background: values with a too high uncertainty ( $var > 0.4$ ) for being considered in the average.

Sub-catalogues	Characteristics				Mmax-aue (Maximum likelihood method)								Mmax aue - obs					
	Data	$Mc$	$M_{max\ obs}$	$M_{max\ obs} + 0.3$	G-K		G-K-B		K-S		K-S-B							
					$M_{max}$	var ( $\pm$ )	$M_{max}$	var ( $\pm$ )	$M_{max}$	var ( $\pm$ )	$M_{max}$	var ( $\pm$ )						
1	1931–1955	39	4.4	6.16	6.4	6.69	0.57	6.58	0.47	6.5	0.39	6.47	0.37	6.3	0.24	6.42	0.33	0.26
2	1956–1965	327	3.7	6.32	6.62	6.82	0.98	6.77	0.49	6.82	0.54	6.66	0.34	6.55	0.3	<b>6.68</b>	0.39	0.38
3	1966–1989	172	4.6	5.7	6	5.78	0.22	5.76	0.21	5.77	0.21	5.76	0.21	5.76	0.21	<b>5.77</b>	0.21	0.07
4	1990–2015	179	4.1	6.2	6.5	6.41	0.22	6.37	0.21	6.4	0.22	6.32	0.2	6.4	0.28	<b>6.38</b>	0.23	0.18
1–4	1931–2015	717	6.32	6.62	6.4	0.22	6.37	0.21	6.38	0.21	6.38	0.21	6.4	0.22	<b>6.39</b>	0.21	0.07	
2–4	1956–2015	678	6.32	6.62	6.39	0.21	6.35	0.20	6.40	0.22	6.38	0.21	6.50	0.27	<b>6.40</b>	0.22	0.08	
3–4	1966–1989	351	6.20	6.50	6.30	0.22	6.26	0.21	6.28	0.22	6.26	0.21	6.41	0.29	<b>6.30</b>	0.23	0.10	
2, 4	1956–1965 1990–2015	506	6.32	6.62	6.41	0.22	6.38	0.21	6.40	0.22	6.38	0.21	6.49	0.26	<b>6.41</b>	0.22	0.09	
Zones																		
1	Virunga	54	4.6	5.4	5.7	5.46	0.12	5.46	0.12	5.46	0.12	5.45	0.11	5.44	0.13	<b>5.45</b>	0.12	0.05
2	Kivu	33	4.6	6.2	6.5	7.65	1.36	7.02	0.83	6.74	0.55	6.66	0.47	6.5	0.32	<b>6.50</b>	0.32	0.30
3	Rusizi	74	4.6	6.3	6.6	6.6	0.3	7.25	0.96	7.02	0.73	6.74	0.45	6.8	0.34	<b>6.70</b>	0.22	0.40
4	Elila	43	4.6	5.8	6.1	5.81	0.1	6.01	0.21	7.1	1.3	6.37	0.58	6.1	0.32	<b>5.97</b>	0.21	0.17
5	Masisi	53	4.6	5.6	5.9	5.81	0.23	5.77	0.2	5.75	0.18	5.73	0.16	5.68	0.13	<b>5.75</b>	0.18	0.15
6	Nyungwe	49	4.6	5.5	5.8	5.71	0.23	5.67	0.2	5.64	0.17	5.63	0.16	5.6	0.14	<b>5.65</b>	0.18	0.15
7	Akagera	49	4.4	6	6.3	6.43	0.44	6.87	0.89	6.61	0.64	6.43	0.47	7.06	1.08			
All zones		306	4.6	6.3	6.6	6.55	0.32	6.44	0.24	6.46	0.26	6.41	0.23	6.45	0.25	<b>6.46</b>	0.26	0.16

have been reported at meteorological stations in this region before the deployment of seismic stations and particularly in the region of Butare in Rwanda. From the processing of these historical data (see above), their magnitude have been estimated between 4.5 and 5.5 (not considered in the seismic hazard assessment). The strongest instrumental event in this zone has a Mw-eq of 5.5 (2003-04-04, ISC catalogue).

At the eastern side the map, the Akagera zone (7) is more stable, but still affected by moderate seismicity. In February 1999, a sequence of events occurred along a NW-trending line starting in the Akagera Park and expanding in a SW direction, south of Kigali with the strongest event (Mw-eq. 6.0) on the 1999-02-15. The events of this sequence are from the Council for Geoscience Catalogue, determined by EAF.

## 5.2. Evaluation of the maximum regional magnitude $M_{\max}$

The magnitude of largest possible earthquake or maximum regional magnitude  $M_{\max}$  for a given seismogenic zone or an entire region is an important parameter in seismic hazard assessment but generally poorly constrained (e.g. McCalpin, 1996; Camelbeeck et al., 2007; Joshi and Sharma, 2008; Kijko, 2004; Kijko and Singh, 2011). Deterministic methods can be used to determine  $M_{\max}$ , based on fault rupture length, strain rate, known activity along active faults, paleoseismic data or probabilistic, based on past seismicity.

The analysis of fault rupture length has been done above for the entire Kivu region (Fig. 4). It gives a rough the evaluation of the  $M_{\max}$  (7.3) that can only be considered as upper bound for the  $M_{\max}$  estimation as the knowledge of the active fault ruptures and their segmentation is insufficient.

The first-order opening velocity of the Kivu rift region has been estimated at between 1.7 and 2.3 mm/yr, based on a rigid plate model and of sparse continuous GPS data and earthquake focal mechanisms (Saria et al., 2014). Furthermore, the distribution of slip between the major rift border faults and the other faults inside the basin is not known. For the entire western rift branch, no paleoseismic data exist on active faults and only a rough estimation of the slip rate for the Kanda fault in the Ufipa plateau between Lakes Tanganyika and Rukwa is available (Delvaux et al., 2007, 2012). In the present case, it is therefore not possible to relate  $M_{\max}$  to the strain rate.

In absence of reliable estimates of the maximum regional magnitude  $M_{\max}$  based on active fault data and strain rate distribution, we will use the catalogue of instrumental earthquakes. Among the possible methods for determining  $M_{\max}$  (Camelbeeck et al., 2007; Kijko, 2004), we considered: (1) addition of a magnitude increment to the maximum observed magnitude, (2) extrapolation of the Gutenberg-Richter cumulative magnitude-frequency distribution to a given return period and (3) estimation using maximum likelihood statistical methods. This was done for the 7 seismotectonic zones defined above, and also for the entire region.

The maximum observed magnitude ( $M_{\max-obs}$ ) ranges from 6.2 to 6.3 in the non-magmatic parts of the rift (Lake Kivu and Rusizi – North Tanganyika zones), 5.4 in the magmatic Virunga - Rutshuru zone, and between 5.6 and 6.0 outside the active rift zone. Conversely, the two other rift segments that do not show evidence for late Quaternary volcanism, are the zones with the largest  $M_{\max-obs}$  in the Kivu region. For evaluating the regional  $M_{\max}$ , an increment of 0.5 is often added to  $M_{\max-obs}$  but we prefer to add only an increment of 0.3. We obtain therefore  $M_{\max-obs+0.3}$  ranging from of 5.7–6.6.

The observation that the  $M_{\max-obs}$  in the Virunga - Rutshuru zone is the lowest for the entire region is compatible with the fact that this segment is affected by late Quaternary magmatism. Dyking

under the northern part of Lake Kivu related to the January 2002 eruption of the Nyiragongo has been inferred by Wauthier et al. (2012), with a 4–11 km deep dyke extending from the Nyiragongo volcano to the northern part of Lake Kivu, up to half way to the northern tip of Idjwi Island. It acted as a magma reservoir feeding the shallow (0–2 km) dyke which was responsible for the eruption. This dyke also possibly induced the 24 October 2002 Mw 6.2 Kalehe earthquake on the western rift flank by Coulomb stress change (Wauthier et al., 2015). Dyke-like conduits are also present beneath the upper southeastern flank of Nyamulagira volcano (Wauthier et al., 2013, 2014). Magma intrusion processes beneath the Virunga area transfer heat to weaken the crust and mantle lithosphere and the volcanic loads flex the plate (Wood et al., 2015), so the combined heating and bending stress lead to reduction in plate strength beneath the Virunga area. In addition, dike intrusions are largely aseismic (Buck, 2006; Calais et al., 2008), potentially leading to smaller percentage of  $M > 4$  earthquakes than in non-magmatic rift sectors (e.g. Belachew et al., 2011), in a magma-assisted extension process.

The evaluation of the regional  $M_{\max}$  is also frequently done by extrapolating the G-R linear fit defined by the a- and b- values, up to a given return period. But this procedure assumes that the G-R relation is valid for all magnitude ranges and also that there is no fixed limit to the highest magnitude. In consequence, the  $M_{\max}$  obtained depends on the assumption on the return period for the highest magnitude earthquake, which is in general not known, and particularly in the Kivu rift. To avoid these problems, maximum likelihood statistical methods have been developed, with different kind of magnitude cumulative distribution functions (Kijko, 2004).

After defining for each zone/catalogue the magnitude of completeness  $M_c$  visually on the G-R plots (Fig. 10), values of  $M_{\max}$  and their uncertainties are computed using the AUE (Aki-Utsu-Extension) MATLAB program of Kijko and Smit (2012), using five different methods: Gibowicz-Kijko (G-K: Gibowicz and Kijko, 1994), Gibowicz-Kijko-Bayes (G-K-B: Kijko and Singh, 2011), Kijko-Sellevoll doubly truncated G-R relationship, (K-S estimator: Kijko and Sellevoll, 1989), Kijko-Sellevoll-Bayes (K-S-B estimator: Kijko, 2004) and the non-parametric Gaussian method (N-P-G: Kijko, 2004). The first four methods follow the Gutenberg-Richter magnitude distribution while the N-P-G method does not assume a specific distribution and is thus independent of the Gutenberg-Richter law. Using tests on synthetic catalogues, Kijko (2004) showed the superiority of the K-S-B and the N-P-G estimates over the K-S estimate.

With these methods, we first computed the  $M_{\max}$  for all the four sub-catalogues and for different combinations of sub-catalogues of different level of completeness. We then computed the  $M_{\max}$  for the seven zones and also for the entire region as a whole using the catalogue extract from 1956 to 2015 with a minimum magnitude of 4.4. In each case, we determined the average estimate  $M_{\max-aue}$  using only results with variance less than 0.4 magnitude unit (Table 2). All calculations have been done with a standard error in magnitude determination of 0.2 for the instrumental catalogue and 0.4 for the mostly historical sub-catalogue (1931–1955).

The results for the sub-catalogues show a fluctuation of the  $M_{\max-aue}$  values for the different periods for the entire region (Table 2, upper part). The third period (1966–1989) shows anomalously low value (5.77) while the three other periods range closely between 6.38 and 6.68. Despite the high uncertainties, the mostly historical sub catalogue 1 (1931–1955) falls within this range with a  $M_{\max-aue}$  of 6.42. The combination of sub-catalogues of different level of completeness gives also similar values: 6.39 for the four catalogues (1931–2015), 6.40 for the last three catalogues (1956–2015), 6.30 for the last two (1966–2015) and 6.41 for the combination of the second (1956–1966) and last catalogues

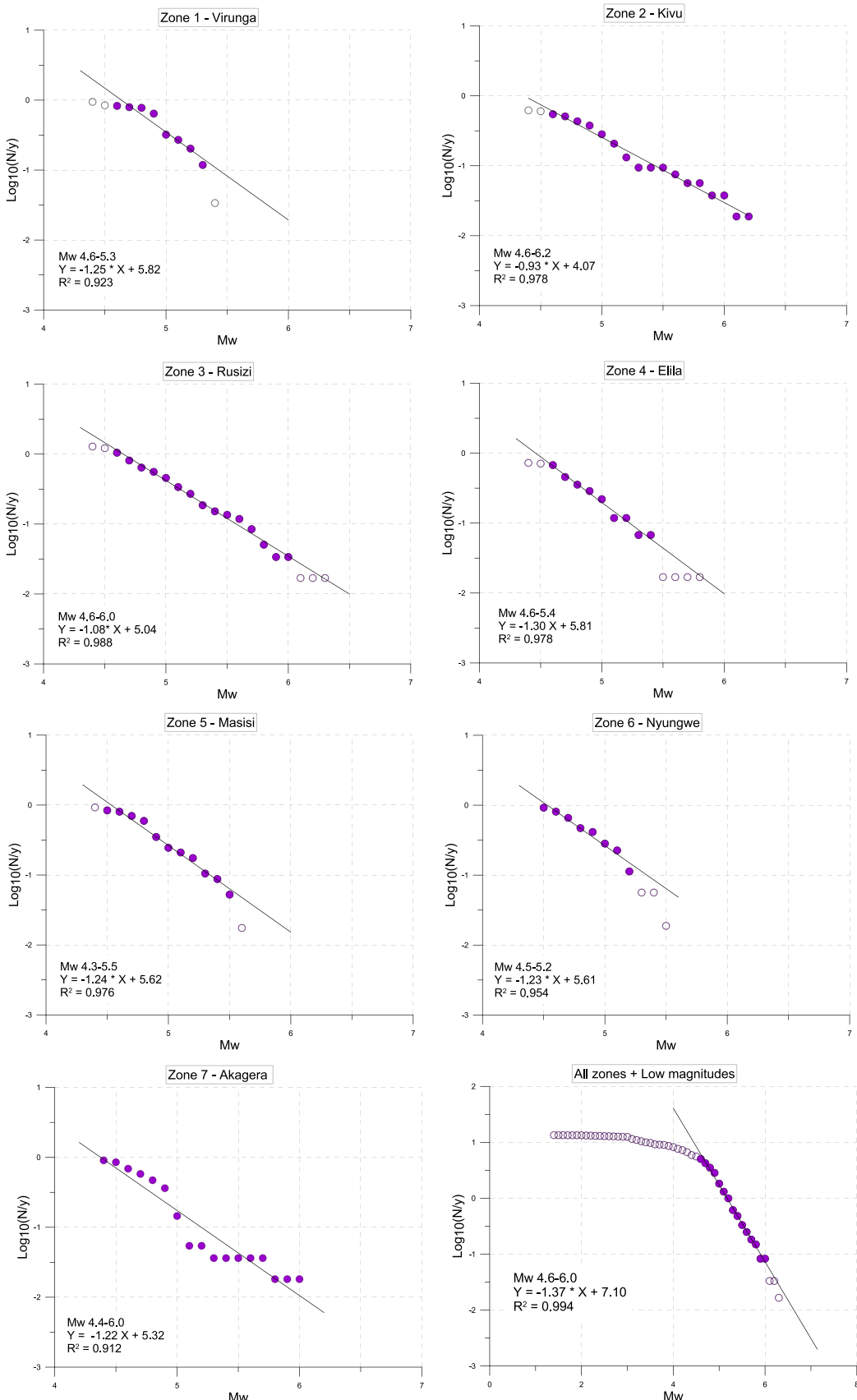


**Fig. 10.** Gutenberg-Richter law analysis and resulting parameters for the 7 seismic zones and all zones grouped together using the declustered catalogue extracted from declustered sub-catalogues 2, 3 and 4, with a common minimum magnitude of 4.4 (1955–2015, 359 data). The data are displayed as in Fig. 8. The number of data per zone is given in Table 1, the Gutenberg and Richter are parameters displayed in Table 3 (lower part).

(1990–2015), skipping the third period (1966–1989) which provides a too high b-value and is apparently incomplete (see below). Using the single catalogue for the entire region (1956–2015,  $M_{eq} \geq 4.4$ ), the  $M_{max-aue}$  obtained is 6.46 for  $M_c = 4.6$ , not significantly different than from the other estimates. For  $M_c = 4.4$ , the  $M_{max}$  obtained by the four methods which depend on the G-R law are about 0.1 unit lower, and the N-P-G independent method presents the same value (6.45).

For the source zones (**Table 2**, lower part), as expected, the  $M_{max-aue}$  for the volcanic Virunga – Rutshuru zone is the lowest (5.45) and those of the Lake Kivu and Ruzizi – North Tanganyika rift zones are the highest (6.5 and 6.7). No  $M_{max-aue}$  average value was obtained for the Akagera zone as the variances obtained with the five methods are also high. We used therefore the value of  $M_{max-obs+0.3}$  (6.3). For the other zones, the  $M_{max-aue}$  values decrease progressively as can be expected from their tectonic setting, from the Kamituga failed rift (Elila: 5.97), the Bukyakiri fault zone (Masisi: 5.75) and the shoaling side of the rift (Nyungwe: 5.65).

It is interesting to note that the difference between the average  $M_{max-aue}$  obtained by the maximum likelihood method and the observed maximum magnitude the  $M_{max-obs}$  is variable (**Table 2**, last column). These values can be compared with the proposed increment of 0.3 as one method to estimate  $M_{max}$ . They range between 0.7 and 0.27 for the individual sub-catalogues and 0.08–0.15 for the combined sub-catalogues. For the source zones this difference appears somehow related to the tectonic setting (and the  $M_{max-aue}$ ): the lowest difference is recorded in the Virunga – Rutshuru volcanic rift zone (0.05) and the highest, in the non-volcanic Rusizi – North Tanganyika (0.41) and Lake Kivu (0.38) rift zones while the other zones (not considering the Akagera zone) have differences of 0.15–0.17 and the entire region (all zones), of 0.15.

### 5.3. Evaluation of the a- and b-values

Similarly we evaluated the a- and b-values using both the least square linear fit to the G-R cumulative plot and the maximum likelihood method (**Fig. 10**; **Table 3**). The least square linear fit was performed between the magnitudes  $M_c$  and  $M_{max-obs}$  if the relation has a good linearity for the highest magnitudes. When the upper magnitudes depart from a good linearity with the lower

magnitudes, we determined the upper limit in an arbitrary way. The maximum likelihood method was performed using the AUE program of [Kijko and Smit \(2012\)](#). It provides unique Lambda- and b-values for all the methods implemented. The activity rate Lambda is given for the magnitude  $M_c$ . It has been extrapolated to  $M = 0$  to obtain the equivalent a-value of the G-R linear fit. According to [Sandrini and Marzocchi \(2007\)](#), the least square technique introduces bias in the estimation of the b-value and the maximum likelihood method is preferred.

For the sub-catalogues (**Table 3**, upper part), the b-values from the AUE program are generally low (0.7–0.8), except for the third period (1966–1989) where it reaches almost 1.47, demonstrating a problematic database for that period. The b-value from the combined catalogues reaches 1.03 when the two most recent sub-catalogues are considered (1966–2015), and 0.94–0.95 otherwise. Combining the second and the last catalogue gives also a low b-value (0.79). The period 1966–1989 clearly appears anomalous relative to the other periods for both the  $M_{max}$  and the b-values, reflecting either the incompleteness of the catalogue, or errors in the determination of the magnitude. This is consistent with the fact that during this period, there has been a marked degradation of the

**Table 4**

Synthesis of the values of the Gutenberg-Richter parameters obtained (**Tables 2** and **3**) and used in the seismic hazard calculations by seismotectonic source zone and for the entire region (all zones). Data: number of data by zone; Mc: Magnitude of completeness; a: activity rate for  $Mw = 0$ ; b: b-value with its variance; Mmax: Maximum magnitude; obs: Mmax observed obs, used: Mmax computed using the maximum likelihood method and with its variance; 475y-aue: Mmax for 475 years return period computed with the a- and b- values obtained with maximum likelihood method; 475y-ls: Mmax for 475 years return period computed with the least-square method.

Zones	Data	Mc	a	b	Mmax			
					obs	used	475y-aue	475y-ls
1 Virunga	55	4.6	5.24	1.16	5.4	5.45	6.82	6.80
2 Kivu	33	4.6	4.01	0.94	6.2	6.50	7.11	7.25
3 Rusizi	76	4.6	5.30	1.15	6.3	6.70	6.94	7.15
4 Elila	43	4.6	5.81	1.30	5.8	5.97	6.10	6.53
5 Masisi	53	4.6	6.19	1.37	5.6	5.75	6.47	6.69
6 Nyungwe	49	4.6	5.61	1.23	5.5	5.65	6.27	6.74
7 Akagera	52	4.4	4.94	1.14	6	6.30	6.68	6.55
All zones	306	4.6	6.69	1.30	6.3	6.46	7.20	7.58

**Table 3**  
Gutenberg-Richter values determined with the determined by the maximum likelihood method using the program AUE of [Kijko and Smit \(2012\)](#) and the least square method. Upper part: for the sub-catalogues, lower part: for the seismotectonic source zones and for the entire region (all zones). Data: number of data by zone; Mc: Magnitude of completeness;  $\lambda$ : activity rate at the magnitude of completeness and its variance; a: (equivalent) activity rate for  $Mw = 0$ ; b: b-value and its variance. For both the maximum likelihood and the least square method, the Mmax for a return period of 475 years (Mmax-475y) is computed with the related a- and b- parameters.

Sub-catalogues	Data	Mc	Maximum likelihood method						Least square method		
			$\lambda$	$\pm$	a	b	$\pm$	Mmax-475y	a	b	Mmax-475y
1 1931–1955	39	4.5	1.32	0.40	3.72	0.80	0.21	8.00	3.21	0.69	8.57
2 1956–1965	327	3.7	9.36	0.25	3.86	0.78	0.04	8.38	4.27	0.83	8.37
3 1966–1989	172	4.6	7.12	1.86	7.61	1.47	0.16	7.00	9.50	1.91	6.36
4 1990–2015	179	4.1	6.92	1.80	4.16	0.81	0.08	8.44	5.71	1.14	7.36
1–4 1931–2015	717	3.7	20.66	3.84	4.79	0.94	0.05	7.95			
2–4 1956–2015	678	3.7	26.28	5.61	4.93	0.95	0.05	8.01	7.10	1.37	7.14
3–4 1966–2015	351	4.1	14.64	3.06	5.39	1.03	0.07	7.83			
2, 4 1956–1965	506	3.7	12.62	2.80	4.02	0.79	0.06	8.48			
1990–2015											
Zones											
1 Virunga	54	4.6	0.80	0.23	5.24	1.16	0.46	6.82	5.82	1.25	6.80
2 Kivu	33	4.6	0.48	0.15	4.01	0.94	0.24	7.11	4.07	0.93	7.25
3 Rusizi	74	4.6	1.03	0.29	5.30	1.15	0.18	6.94	5.04	1.08	7.15
4 Elila	43	4.6	0.67	0.20	7.51	1.67		6.10	5.81	1.30	6.53
5 Masisi	53	4.6	0.77	0.22	6.19	1.37	0.34	6.47	5.62	1.24	6.69
6 Nyungwe	49	4.6	0.72	0.21	6.85	1.52		6.27	5.61	1.23	6.74
7 Akagera	49	4.4	0.83	0.24	4.94	1.14	0.21	6.68	5.32	1.22	6.55
All zones	306	4.6	5.10	1.31	6.69	1.30	0.09	7.20	7.71	1.37	7.58

seismic networks and the recorded seismicity appears incomplete, even above  $M_c = 4.6$ . A similar trend is observed for the b-values obtained from the linear fit, with even greater differences.

For the source zones (Table 3, lower part), b-values from respectively the AUE program and from the linear fit are relatively similar for the entire region (1.30/1.37) as for the other zones, except for Nyungwe (1.52/1.23) and Elila (1.67/1.30) zones. For these two zones, the maximum likelihood method provide anomalously high b-values and is not able to provide uncertainties for the a- and b-values. For all zones, average to high b-values (0.9–1.3) were obtained. Such values are characteristic for regions marked by a comparatively large weight of small seismic events. This result is confirmed by the absence of any  $M > 7$  event in the region within the observation period (starting at the end of the 19th century), while M-6 events are relatively common. Compared to Déprez et al. (2003) for the central part of the western rift branch, we obtained also b-values close or higher than 1.0 (1.15–1.30).

Using these a- and b-values, the  $M_{max}$  values are extrapolated for the standard return period of 475 years ( $M_{max-475y}$ ). These are much higher than the average  $M_{max-aue}$  values by 1–2.5 magnitude units for the sub-catalogues and 0.1–1.37 for the source zones.

## 6. Seismic hazard evaluation

For the seismic hazard evaluation, we used when possible the average  $M_{max-aue}$  values and the a- and b-values determined by the maximum likelihood methods implemented in the AUE program (Table 3). For the Akagera zone, for which the uncertainties in the  $M_{max-aue}$  are too high, we incremented the maximum observed magnitude ( $M_{max-obs}$ ) by 0.15, the calculated difference between  $M_{max-aue}$  and  $M_{max-obs}$  for the adjacent zones. For the Elila and Nyungwe zones, we used the least square a- and b-values as explained above.

### 6.1. Existing attenuation models

It was not possible to derive new specific Ground Motion Parametric Equations for the project area because of the lack of accelerometric data for known earthquakes in the region. We used therefore the existing attenuation laws of Jonathan (1996) developed for southern and eastern Africa, Twesigomwe (1997) developed for Uganda and the law of Mavonga (2007) developed for the Kivu rift region:

$$\ln(a_1) = 3.024 + 1.030 \text{ Mw} - 1.351 \ln(\text{Rh}) - 0.0008 \text{ Rh} \quad (\text{Jonathan, 1996})$$

$$\ln(a_1) = 2.832 + 0.866 \text{ Mw} - \ln(\text{Rh}) - 0.0025 \text{ Rh} \quad (\text{Twesigomwe, 1997})$$

$$\ln(a_2) = -6.5386 + 1.43 \text{ Mw} - 1.5 \ln(\text{Re}) \quad (\text{Mavonga, 2007})$$

with  $a_1$  in  $\text{cm/s}^2$  and  $a_2$  in 'g' (the results in 'g' by the law of Mavonga, 2007; were multiplied by 981), where Mw is here the moment-magnitude and Rh and Re are the hypocentral and epicentral distances, respectively.

A comparison between results obtained applying those three laws is shown in Fig. 11. It shows that the law of Mavonga (2007) produces the strongest attenuation (lowest acceleration at larger distances), the one of Jonathan (1996) produces intermediary results and the one of Twesigomwe (1997) the lowest attenuation (largest acceleration at larger distance). However, at very short distance, the two first laws (Mavonga and Jonathan) produce the highest acceleration values. Both the Jonathan (1996) and Twesigomwe (1997) laws are dependent on the hypocentral distance, and they are therefore sensitive to the hypocentral depth determination for short distances. Here, the average hypocentral

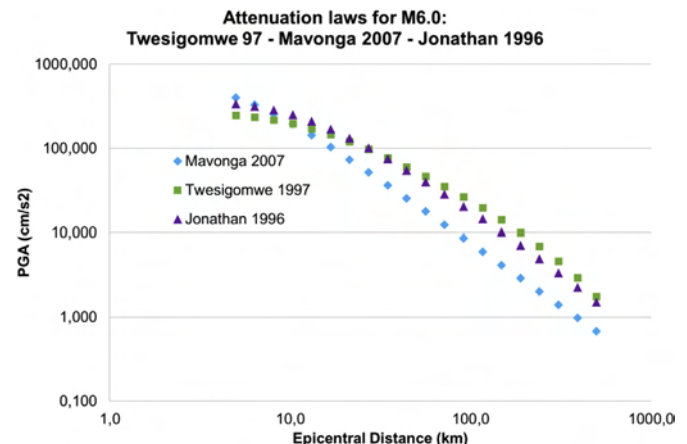


**Fig. 11.** Detailed comparison between acceleration values calculated with the applied Mavonga (2007), Twesigomwe (1997) and Jonathan (1996) attenuation laws for a  $M_w = 6.0$  event, considering an average hypocentral depth of 11 km for the two latter laws.

depth is estimated at 11 km according to the most frequent focal depth between 10 and 12 km as discussed above.

We used these three laws to provide various estimates of seismic hazard for the region as we do not know a priori which law is more suitable. Below it will be seen that the different acceleration values obtained by these laws at medium and large epicentral distances will strongly constrain the seismic hazard calculation results.

### 6.2. Probabilistic seismic hazard computation

On the basis of the G-R parameters obtained for each sources zone (Table 4) and the three attenuation laws selected, we computed probabilistic seismic hazard maps for the area with the CRISIS2012 software for probabilistic seismic hazard analysis (Ordaz et al., 2013).

The three maps obtained (Fig. 12) display different levels and patterns of peak ground acceleration (PGA). In general, the map computed with the Mavonga (2007) attenuation law (Fig. 12a) shows the lowest PGA values (for 475-year return period) of 0.17–0.32 g along the axis of the western branch of the East African Rift, while the map produced with the Jonathan (1996) law (Fig. 12c) presents the highest PGA values (0.25–0.43 g). The map produced with the Twesigomwe (1997) law presents similar minimum values (0.28 g) but lower maximal values (up to 0.37 g).

For all three maps, the central rift zone presents contrasting PGA values, with the highest in the currently non-magmatic part of the Kivu basin (zone 2) and the lowest in the volcanic northern extremity of the Kivu Basin, Virunga volcanic massif and Rutshuru basin (zone 3). Similarly, the Nyungwe zone (6) has relatively similar PGA as for the central Vurunga-Rutshuru zone (1): 0.17–0.20 g with the Mavonga (2007) attenuation law and 0.21–0.30 g with the two other laws. For the three lateral zones, the Mavonga (2007) attenuation law gives similar low PGA values (0.10–0.16), while the two other laws give a gradation of PGA values with the highest (0.21 g) for the Kamituga failed rift (zone 4), intermediate (0.18 g) for the Bunyakiri fault zone (5) and the lowest (0.08–0.16 g) for the Akagera zone (7).

According to the IASPEI seismic hazard classification (Lee et al., 2003), the non-magmatic central rift zone would be marked by high peak ground acceleration values (0.24–0.40 g after IASPEI) and the lateral zones, together with the magmatic part of the rift, by moderate peak ground acceleration values (0.08–0.24 after IASPEI). The seismic hazard is systematically higher in the central part of the

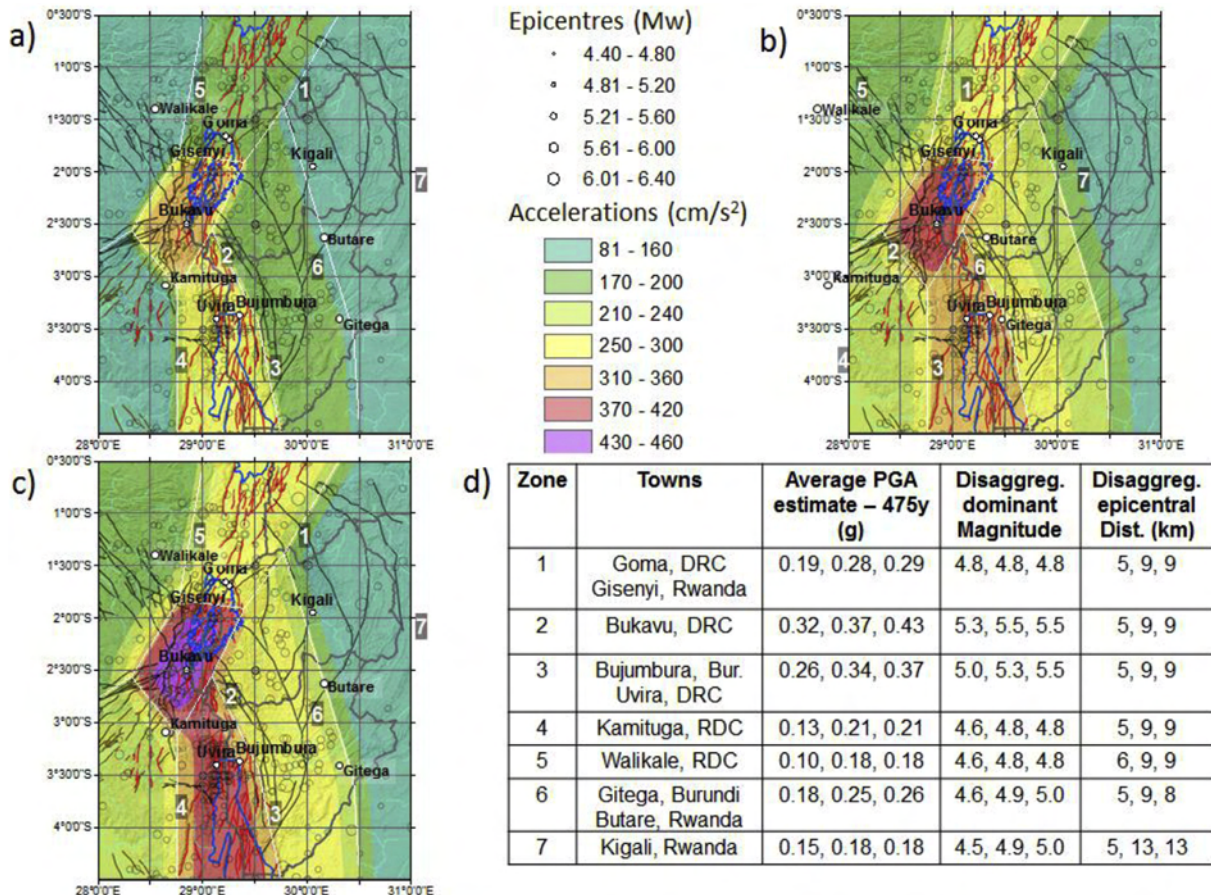


**Fig. 12.** Seismic hazard assessment results for the central target area, for a 475-year return period in terms of Peak Ground Acceleration (PGA) on the bedrock: computation with the attenuation law of a): Mavonga (2007); b): Twesigomwe (1997); c): Jonathan (1996). On all maps are plotted also the main seismic shocks (circles with size according to magnitude), country borders, contour of Lake Kivu (in blue) and main cities. d) Averaged 475-year PGA estimate for cities in the target area with indication of the dominant magnitude-epicentral distance pair provided by the disaggregation charts: 3 values of Magnitude and epicentral distance, respectively, for each town, corresponding to results obtained for the 3 attenuation laws. (For interpretation of the references to colour in this figure legend, the reader is referred to the web version of this article.)

rift (Lake Kivu zone). For this area, the estimates based on the attenuation law by Jonathan (1996) even predict very high peak acceleration values (>0.40 g after IASPEI).

At present, we cannot clearly state which of the three maps (Fig. 12a–c) reproduces the most likely situation as we do not possess any measured acceleration data that could validate one of the three attenuation laws used, which is here the only changing component. We consider that with the given uncertainties, it is not possible at present to provide a more reliable seismic hazard assessment and the values obtained with the three models should be considered as minimum (with Mavonga, 2007), intermediate (with Twesigomwe, 1997) and maximum (with Jonathan, 1996).

## 7. Discussion

### 7.1. Sources of uncertainties

The main sources of uncertainty for our estimates of the seismic hazard are the relatively short observation period, the inhomogeneity of the seismic catalogue, uncertainties in the magnitude determination, epicentral location and hypocentral depth of earthquake, the definition of the seismic zoning and the missing peak ground acceleration data.

The first three uncertainties affect the Gutenberg-Richter magnitude-frequency distribution. They can only be reduced by enlarging the observation period and densifying the seismic observatories. Reprocessing the seismic data from the IRSAC network

might also improve the quality of the data for the 1956–1965 period. These uncertainties are particularly high outside the rift areas as there the seismicity is low and sparse. Within the rift zone, the number of seismic events is larger and we are more confident about the defined a- and b-values and thus about the final seismic hazard estimates.

The uncertainty in the  $M_{\max}$  estimation affects mainly the long return periods, but has negligible effect for PGA of 10% probability (475 years return period). Sensitivity tests show that the final estimates of the Gutenberg-Richter parameters have a relatively limited impact on the seismic hazard assessment outputs for this standard period of 475 years but become significant for longer return periods of 1000 or 2000 years. To show the relatively negligible influence of the  $M_{\max}$  used for the 475-year PGA estimates we present (table in Fig. 12d) seismic hazard disaggregation results for the major cities in each zone of the studied region: Goma, Bukavu, Uvira, Kamituga, Walikale (DRC), Bujumbura and Gitega (Burundi) and Gisenyi, Kigali and Butare (Rwanda). These results show that magnitudes systematically lower than the observed maximal magnitudes  $M_{\max-obs}$  are most strongly contributing to the final PGA estimates, even for the highest seismic hazard area around Bukavu. The disaggregation analysis also shows that especially events at short epicentral distances (<10 km) contribute to seismic hazard outputs.

The arbitrary definition of the seismic zones may add also significant uncertainties. Mavonga and Durheim (2009) tested two different source models: one with a single zone for the entire

western rift branch and another with four zones for the western rift branch, with different activity rate  $\lambda$  (and a-value) and maximum magnitude  $M_{\max}$  but with similar b-value, considering that they are all in a similar tectonic setting. They found that the two models did not differ significantly. Here, we consider instead that even at the scale of the Kivu rift region, the tectonic setting varies along the trend of the rift (magmatic and non-magmatic segments) as well as laterally (margin of cratonic blocs, failed rift, fault zone ...). The b-value, which explains the mechanical behaviour of the crust, is therefore allowed to vary and was calculated for each zone in order to reflect the diversity of the tectonic setting and its spatial variability. The obtained  $M_{\max}$  values (Table 3) appear coherent with the geological characteristics of the source zones.

Another important source of uncertainty comes for the choice of the attenuation laws. Ideally, it should be validated by ground motion measurements in the study region but such data are clearly missing here.

## 7.2. Comparison with existing models

Considering all those uncertainties (and the absence of validation of attenuation laws), the novel contributions of the present seismic hazard assessment of the region relative to the previous models using seismic source zones (Mavonga and Durrheim, 2009; Midzi et al., 1999) are present at most levels of the seismic hazard assessment. We produced a homogeneous basement tectonic map for the region, which was previously lacking. The revision of the neotectonic setting for the central part of the western rift branch, allowed to differentiate more precisely the active rift valley into

magma-rich and magma-poor segments, to identify a failed rift branch (Kamituga) and an old reactivated fault zone (Bunyakiri) on the western side of the rift. The finer seismic source zoning better reflects their tectonic setting, each characterized by their own set of a- and b-values and  $M_{\max}$ . A new and longer seismic catalogue was produced on the basis of the reviewed ISC catalogue, supplemented by data from other catalogues and new historical data. The G-R parameters were computed using two different methods: least square and maximum likelihood. The average seismic source depth was revised using well constrained events by waveform-modelling. Three different attenuation laws were used as end-members for computing seismic hazard maps.

Our maps show overall larger PGA values than the previous estimates by Mavonga and Durrheim (2009) and Midzi et al. (1999). We obtained for the entire region, up to 0.32 g with the Mavonga (2007) law; 3.8 g with the Twesigomwe (1997) law and 0.43 g with Jonathan (1996) law, while Mavonga and Durrheim (2009) obtained up to 0.15 g (Fig. 13) and Midzi et al., up to 240 cm/s<sup>2</sup> or ~0.24 g (Fig. 14). For large cities such as Goma, Bukavu, Uvira, Gisenyi and Bujumbura in the rift zone, 475-year return period PGA values predicted by the present study are in the range of 0.29–0.43 g depending on the attenuation law, placing these cities in a high seismic hazard zone while previous estimates are in the range of 0.15–0.24 g. For Kigali, the two previous studies both predict about 0.1 g as 475-year return period PGA, while according to our study it could be between 0.15 and 0.18 g, placing this city in a moderate seismic hazard zone instead of a low seismic hazard zone.

We suspect that the higher PGA/acceleration values obtained in this study compared with the Midzi et al. (1999) and Mavonga and

## The effect of refinement of seismic zonation

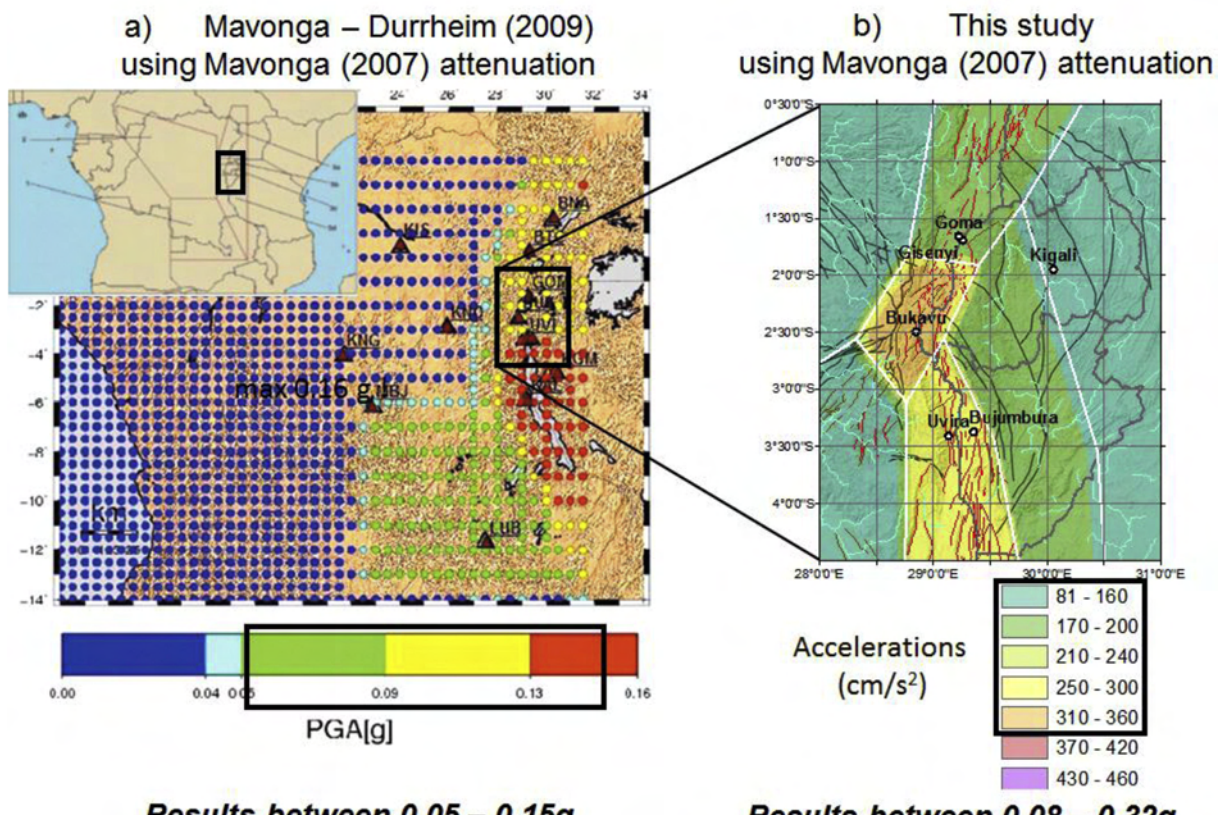


**Fig. 13.** Seismic hazard assessment results (475-year return period) obtained with the Mavonga (2007) attenuation law (b), compared with the map of Mavonga and Durrheim (2009) based on a rougher zonation (a). Black rectangles in a) outline our target area in b).

## Comparison with GSHAP 1999 results

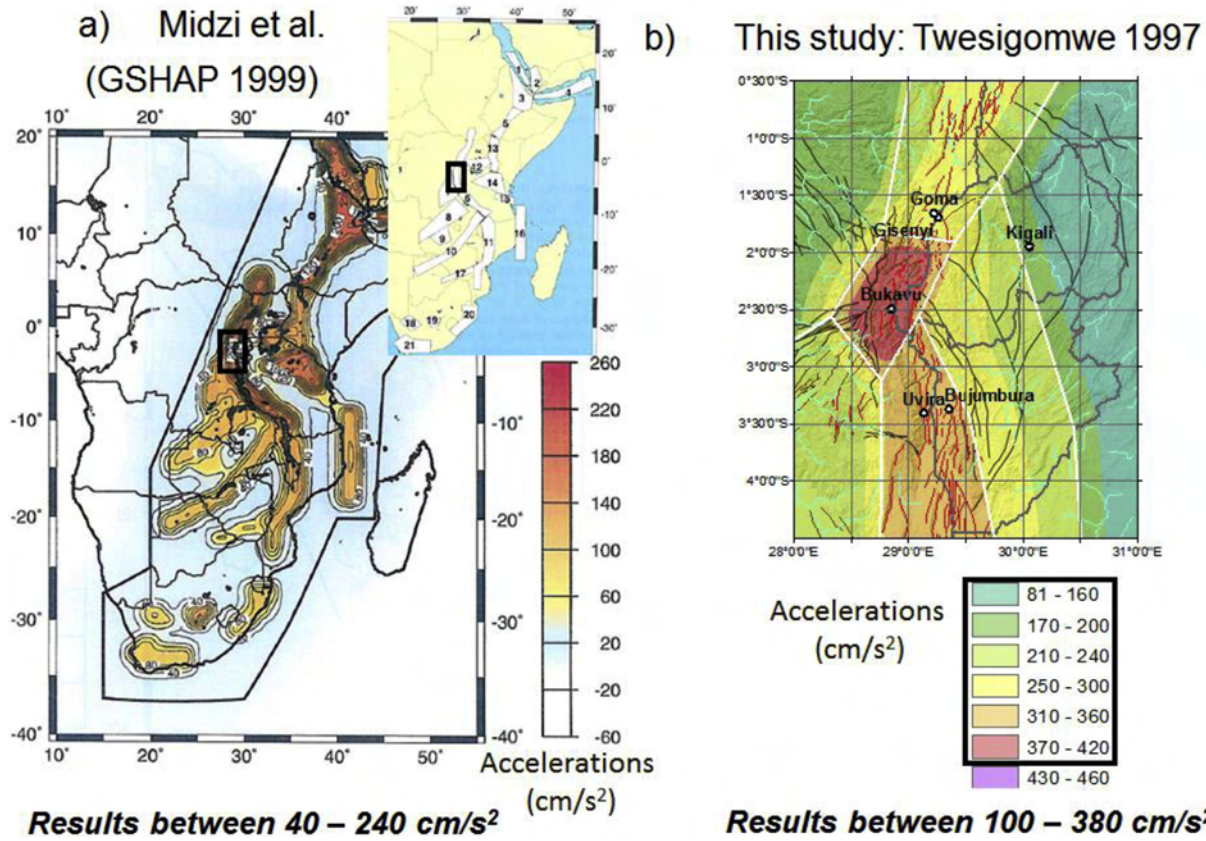


**Fig. 14.** Seismic hazard assessment results (475-year return period) obtained with the [Twesigomwe \(1997\)](#) attenuation law (b) compared with the map of [Midzi et al. \(1999\)](#) for East Africa (GSHAP 1999 model). Black rectangles in a) outline our target area in b).

Durrheim (2009) can be, at least partly, due to a finer seismic zonation. These two previous studies have a much larger extent than ours and the related seismic zonation is clearly rougher than what is proposed here. However, the comparison is not straightforward as these maps were obtained by combining several attenuation laws in a logic tree approach with the EZ-Frisk software package while we used the CRISIS2010 software without a logic tree approach.

Our seismic hazard maps can also be compared with the general map produced by Kijko (2008) for Sub-Saharan Africa based on the maximum likelihood principle, using the K-S and K-S-B estimators and a similar process for computing the PGA, but without defining seismic zones, thus removing this uncertainty on seismic zoning. They also obtain for our region a PGA with 10% probability of exceedance in a 50-year period (equivalent to a return period of 475 years) up to 0.20 g.

### 7.3. Need for seismic monitoring accelerometric data and microzonation studies

Notwithstanding all uncertainties affecting the present study, the seismic hazard could be significantly higher in the western branch of the East African Rift than previously estimated. To confirm these last results, more ground motion data and a longer observation period for the seismicity are required, thus more efforts need to be put into the installation of seismic stations both within the Rift valley and outside. Only when sufficiently seismometric and accelerometric data are available, the uncertainties affecting the hypocenter depths and the attenuation of accelerations over small and large epicentral distances could be reduced. Different methods for computing the seismic hazard should also be performed using the same data set, parameters, zonation and

attenuation laws to isolate the effect of the hazard computation method. Furthermore, the relatively high PGA values for major cities in the region clearly demand more intensive seismic microzonation studies applied to these densely inhabited and strongly changing environments with exponential increase of construction activity, such as in Kigali, Bukavu or Bujumbura.

## 8. Conclusions

A new probabilistic seismic hazard assessment has been performed for the Kivu rift region in the central part of the western branch of the East African rift system. We performed a seismic source zoning on the basis of new tectonic and a new homogeneous tectonic map of the basement across the political borders and a revised neotectonic map which combines the known late-Cenozoic faults, late Quaternary volcanic centers, thermal springs and seismic epicenters. The studied region was subdivided into 7 seismic source zones that reflect the lateral variation of the tectonic setting. The active Kivu rift valley is differentiated into a magma-rich segment (Virunga - Rutshuru) and two magma-poor segments (Lake Kivu and Rusizi - North Tanganyika). On the western side of the rift valley and as a transition towards the intra-continental Congo Basin, we identified the Kamituga failed rift branch which initially formed as the south-westwards continuation of the Lake Kivu basin, and the old reactivated Bunyakiri fault zone on the western side of the rift, in the Masisi region.

A new and longer seismic homogenized catalogue comprising 1068 entries, spanning 127 years from 1888 to 2015 was produced on the basis of the Reviewed ISC catalogue, supplemented by data from other catalogues and new historical data. After declustering and magnitude homogenisation, we obtained a final catalogue of 359

events spanning 60 years (1955–2015) and with a magnitude of completeness of 4.4 over the entire region. The seven seismotectonic source zones are each characterized by their own set of Gutenberg-Richter computed with both the least square and maximum likelihood procedures. An average seismic source depth of 11 km was defined using events constrained by waveform-modelling.

Three attenuation laws were used as end-members for computing seismic hazard maps with the CRISIS 2012 software. We obtain higher PGA values than previous estimates, with maximum PGA values between 0.32 and 0.43 g in function of the attenuation law used, compared to the previous 0.15–0.24 g. This difference might be due to a combination of the effects of a revised and longer earthquake catalogue, finer source zonation with independent calculations of  $a$ -,  $b$ - and  $M_{max}$  values, the relatively shallow hypocentral depth used, the choice of attenuation laws and different calculation methods using different softwares. We consider that the best approximation of the seismic hazard is provided by the model obtained with the [Mavonga \(2007\)](#) and [Twesigomwe \(1997\)](#) attenuation laws, which should be considered respectively as minimum and maximum estimates. The [Jonathan \(1996\)](#) law, which was obtained for the more stable region of South Africa, typically produces a too low attenuation (and too high PGA values) for our region dominated by rifting processes.

These results should be considered as preliminary, given the

limitations of the data set. They need to be confirmed with longer observation period for the seismicity and locally measured ground motion data.

## Acknowledgements

This work has been performed mainly in the frame of project GeoRisCA (Geo-Risks in Central Africa), funded by the Belgian Science Policy (Belspo). The compilation of the catalogue of felt seismic and the determination of macroseismic epicenters have been performed under the project S1\_RDC\_GEOODYN, funded by the Belgian Development Cooperation and managed by the Royal Museum for Central Africa. This work is also a contribution to the UNESCO project IGCP601 Seismotectonics and Seismic Hazards in Africa and the Seismotectonic Map of Africa project of the Organisation of the African Geological Surveys. We thank also C. Ebinger and an anonymous reviewer for helping us to improve the manuscript.

## Appendix A. Epicenter, hypocentral depth and focal mechanism data for available earthquakes processed by waveform modelling.

Date	Time	Long_E	Lat_N	Depth	Magnitude	Strike1	Dip1	Slip1	Strike2	Dip2	Slip2	Shmax	Reference
1967-10-14	23:29:00	28.200	-3.300	10.0	5.1	Mb	142	70	-125	026	40	-032	174
1977-01-06	18:33:42	28.656	-2.542	13.9	5.1	Mw	241	45	-090	061	45	-090	61
1980-01-09	14:50:00	27.619	-3.298	15.0	5.2	Mw	045	48	-142	107	63	-049	76
1981-07-30	16:46:19	28.560	-2.681	15.0	5.1	Mw	235	45	-090	055	45	-090	55
													<a href="#">Kebude and Kulhanek, 1991</a> ; location from ISC
1982-07-03	23:21:12	28.812	-3.829	15.0	5.3	Mw	328	50	-136	206	58	-049	177
1985-06-28	22:46:20	28.944	-2.372	10.0	4.9	Mw	211	45	-090	031	45	-090	31
1986-06-29	21:48:00	29.760	-4.960	36.0	5.6	Mw	191	81	-072	127	20	-153	159
1990-09-04	01:48:01	29.164	-0.375	10.0	5.3	Mw	229	77	006	138	84	167	3
1995-04-29	11:50:54	28.516	-1.310	10.0	5.4	Mb	229	22	-055	012	72	-103	030
													<a href="#">Barth et al., 2007</a> ; location from ISC catalogue, Depth from <a href="#">Mavonga, 2007</a>
2000-03-02	02:44:56	28.265	-2.537	10.0	5.4	Mw	184	47	-060	144	51	-118	164
													<a href="#">Yang and Chen, 2010</a> ; <a href="#">Barth et al., 2007</a> ; location from ISC catalogue
2000-03-02	04:29:50	28.144	-2.380	10.0	4.7	Mb	033	75	-103	255	20	-050	054
2000-03-03	05:03:22	28.153	-2.398	10.0	4.6	Mb	037	83	-137	121	47	-009	079
2002-01-20	00:14:48	28.991	-1.730	10.0	5.1	Mw	039	49	-042	160	60	-130	9
2002-01-21	04:39:25	29.014	-1.728	15.0	5.1	Mw	018	26	-128	239	70	-073	38
2002-01-22	15:32:09	29.033	-1.664	15.0	5.2	Mw	233	26	-043	003	73	-110	29
2002-10-24	06:08:43	29.050	-1.951	8.0	6.2	Mw	209	47	-82	17	44	-99	23
2002-10-24	07:12:18	29.005	-1.838	3.0	5.5	Mw	210	42	-75	10	50	-103	20
2003-03-20	06:15:23	29.507	-2.440	7.0	5.2	Mw	017	45	-023	124	74	-133	160
													<a href="#">Yang and Chen, 2010</a> <a href="#">Craig et al., 2011</a> ; location from ISC catalogue
2003-08-05	18:56:54	29.663	-0.693	15.0	5.2	Mw	330	34	-155	219	76	-059	5
													<a href="#">Craig et al., 2011</a> ; location from ISC catalogue
2008-02-03	07:34:13	28.740	-2.450	8.0	6.0	Mw	350	52	-101	188	39	-76	179
2008-02-03	10:56:10	28.940	-2.420	12.0	5.0	Mw	352	43	-102	188	48	-79	180
2008-02-14	02:07:47	28.850	-2.250	12.0	5.3	Mw	332	69	-121	211	37	-37	2
2008-04-20	07:30:44	25.970	-3.660	26.0	5.2	Mw	207	75	-180	117	89	-15	72

(continued on next page)

(continued)

Date	Time	Long_E	Lat_N	Depth	Magnitude	Strike1	Dip1	Slip1	Strike2	Dip2	Slip2	Shmax	Reference
2008-09-15	15:50:51	30.128	-4.982	10.1	5.1	Mw	138	83	173	229	83	7	3
2008-10-05	00:02:12	29.066	-1.206	9.0	5.3	Mw	347	41	-131	216	60	-60	12
2010-01-28	23:52:30	29.199	-0.945	14.0	4.9	Mw	15	43	-80	181	48	-99	8
2012-12-24	14:35:33	28.393	-4.036	23.4	5.0	Mw	355	37	-107	196	55	-78	5
2013-11-30	19:20:17	27.001	-0.943	15	5.5	Mw	242	88	-179	152	89	-2	107
2015-08-07	01:28:41	28.760	-2.110	31.0	5.5	Mw	204	43	-110	050	50	-072	37
2015-08-07	01:25:02	28.888	-2.161	7.0	5.8	Mw	194	58	-119	60	42	-52	37
2016-02-04	12:43:59	28.430	-1.550	10.0	4.8	Mw	95	040	-90	276	40	-088	95

Source data indicated in the reference column. Harvard CMT: Harvard Centroid Moment Tensor catalogue, ISC: International Seismological center (UK), USGS: United States geological Survey.

## Appendix B. Definition of acronyms of seismic agencies from which the data have been used in the compiled seismic catalogue

### Annexe 2: Acronyms of seismic agencies:

- ISC: International Seismological Centre, United Kingdom
- BUL: Goetz Observatory, Zimbabwe
- EAF: East African Network
- ENT: Geological Survey and Mines Department, Uganda
- GFZ: Helmholtz Centre Potsdam GFZ German Research Centre For Geosciences, Germany
- HARV: Harvard University, U.S.A.
- LSZ: Geological Survey Department of Zambia, Zambia

- LWI: Centre de Géophysique du Zaïre, Democratic Republic of the Congo, hosted by the IRSAC (Institut pour la Recherche Scientifique en Afrique Centrale)
- NAI: University of Nairobi, Kenya
- NEIC: National Earthquake Information Center U.S.A.
- USGS: United States Geological Survey, U.S.A.
- PRE: Council for Geoscience, South Africa

## Appendix C. Macroseismic epicenters and estimated magnitude determined from the catalogue of felt seisms initiated by [Herrick \(1959\)](#) and completed within this work.

ID	Year	Month	Day	Hour	Min	Long E	Lat N	Nsta	Mw-eq
KIV19311206-04:47	1931	12	06	04	47	29.75	-2.15	6	4.67
KIV19320202-10:53	1932	02	02	10	53	29.99	-2.80	6	4.41
KIV19320713-10:40	1932	07	13	10	40	29.75	-2.25	7	4.70
KIV19320903-05:05	1932	09	03	05	05	31.18	-0.73	7	5.12
KIV19320908-15:30	1932	09	08	15	30	29.67	-3.67	4	4.42
KIV19330224-17:00	1933	02	24	17	00	29.89	-3.40	4	4.24
KIV19340115-14:48	1934	01	15	14	48	29.77	-3.43	5	4.48
KIV19340220-19:10	1934	02	20	19	10	29.80	-3.15	4	4.61
KIV19341028-04:42	1934	10	28	04	42	29.72	-2.20	10	4.69
KIV19350206-07:12	1935	02	06	07	12	29.77	-3.15	9	4.60
KIV19350323-05:36	1935	03	23	05	36	30.89	-0.05	8	5.45
KIV19360817-13:12	1936	08	17	13	12	29.51	-2.55	10	4.81
KIV19370728-06:55	1937	07	28	06	55	29.89	-3.30	4	4.30
KIV19380921-11:01	1938	09	21	11	01	29.57	-0.34	4	5.43
KIV19391128-14:03	1939	11	28	14	03	30.21	-3.09	5	4.41
KIV19391218-01:28	1939	12	18	01	28	29.71	-2.65	23	4.82
KIV19400702-13:22	1940	07	02	13	22	29.64	-2.78	18	4.93
KIV19400911-22:52	1940	09	11	22	52	29.79	-2.33	7	4.78
KIV19401024-00:20	1940	10	24	00	20	30.02	-2.87	5	4.63
KIV19401226-17:05	1940	12	26	17	05	29.10	-0.94	4	4.51
KIV19410112-02:30	1941	01	12	02	30	29.34	-2.35	8	4.60
KIV19420226-00:00	1942	02	26	00	00	29.96	-1.19	5	5.38
KIV19420827-15:59	1942	08	27	15	59	28.90	-2.37	5	4.33
KIV19421212-05:20	1942	12	12	05	20	29.69	-1.76	8	4.55
KIV19430331-03:55	1943	03	31	03	55	29.70	-0.37	4	5.32
KIV19430625-03:50	1943	06	25	03	50	29.17	-3.22	5	4.75
KIV19431011-22:05	1943	10	11	22	05	29.65	-2.55	6	4.90
KIV19440519-15:30	1944	05	19	15	30	30.00	-3.20	5	4.45
KIV19450315-13:48	1945	03	15	13	48	29.69	-3.39	4	4.41
KIV19450318-09:58*	1945	03	18	09	58	29.91	-0.86	15	6.00
KIV19520306-15:32	1952	03	06	15	32	30.10	-3.28	4	4.47
KIV19520404-20:16*	1952	04	04	20	16	29.98	-2.95	8	4.61
KIV19530421-04:16	1953	04	21	04	16	29.79	-3.29	5	4.50
KIV19531109-13:21*	1953	11	09	13	21	29.54	-3.03	4	4.63
KIV19540822-06:33	1954	08	22	06	33	30.13	-3.23	6	4.42
KIV19541216-12:38	1954	12	16	12	38	30.01	-3.31	7	4.49
KIV19550227-01:39	1955	02	27	01	39	29.94	-3.39	5	4.45

(continued)

ID	Year	Month	Day	Hour	Min	Long E	Lat N	Nsta	Mw-eq
Equivalent events from ISC									
KIV19450318-08:01	1945	03	18	08	01	32.00	0.00		6.00
KIV19520404-20:09	1952	04	04	20	09	29.73	-4.23		4.60
KIV19531109-14:04	1953	11	09	14	04	28.50	-4.00		4.60

Long\_E: longitude (positive eastwards). Lat\_N: latitude (positive northwards, here negative southwards). Mag: estimated magnitude from the perception distance determined from the data of Ambraseys (1991) on the Rukwa 1910 seismic sequence. Nch: number of felt shocks recorded. Nst: Number of different stations that recorded the felt shocks.

## Appendix D. Supplementary data

Supplementary data related to this article can be found at <http://dx.doi.org/10.1016/j.jafrearsci.2016.10.004>.

## References

- Adams, A., Nyblade, A., Weeraratne, D., 2012. Upper mantle shear wave velocity structure beneath the East African plateau: evidence for a deep, plateau wide low velocity anomaly. *Geophys. J. Int.* 189 (1), 123–142.
- Ambraseys, N.N., 1991. The Rukwa earthquake of 13 December 1910 in East Africa. *Terra Nova* 3, 202–211.
- Ambraseys, N.N., Adams, R.D., 1986. Seismicity of the Sudan. *Bull. Seismol. Soc. Am.* 76, 483–493.
- Ambraseys, N.N., Adams, R.D., 1991. Reappraisal of major African earthquakes, south of 20°N, 1900–1930. *Nat. Hazards* 4, 389–419.
- Bäth, M., 1965. Lateral inhomogeneities in the upper mantle. *Tectonophysics* 2, 483–514.
- Barth, A., Wenzel, F., Giardini, D., 2007. Frequency sensitive moment tensor inversion for light to moderate magnitude earthquakes in eastern Africa. *Geophys. Res. Lett.* 34 (L15302).
- Belachew, M., Ebinger, C., Coté, D., Keir, D., Rowland, J.V., Hammond, J.O.S., Ayele, A., 2011. Comparison of dike intrusions in an incipient seafloor-spreading segment in Afar, Ethiopia: Seismicity perspectives. *J. Geophys. Res.* 116, B06405. <http://dx.doi.org/10.1029/2010JB007908>.
- Biayi-Kalala, W., 1984. Contribution à l'étude du magmatisme alcalin du massif du Kahuzi (Kivu, Zaïre). Ph.D. Thesis. Lab. Aardkunde, University of Gent, Belgium, p. 246, 2 maps.
- Biggs, J., Chivers, M., Hutchinson, M.C., 2013. Surface deformation and stress interactions during the 2007–2010 sequence of earthquake, dyke intrusion and eruption in northern Tanzania. *Geophys. J. Int.* 195, 16–26.
- Boutakoff, N., 1933. Les sources thermo-minérales du Kivu, leurs relations avec les grandes fractures radiales et leur utilisation au point de vue tectonique. *Bull. Soc. Belge. Géol.* 43, 75–80.
- Boutakoff, N., 1939. Géologie des terrains situés à l'Ouest et au Nord-Ouest du fossé tectonique du Kivu, IX(1). *Mém. Inst. Geol. Univ. Louvain*, pp. 1–207.
- BRCM, 1982. Carte géologique du Haut Zaïre et du Nord Kivu au 1/500.000. Département des Mines, Service géologique. Feuille Nord-Kivu, République du Zaïre.
- Brinckmann, J., Lehmann, B., Hein, U., Höhndorf, A., Mussallam, K., Weiser, T., Timm, F., 2001. La géologie et la minéralisation primaire de l'or de la chaîne Kibarienne, Nord-Ouest du Burundi, Afrique orientale. *Geol. Jarhb. D101*, 3–195.
- Buck, W.R., 2006. The role of magma in the development of the Afro-Arabian Rift System. In: Yirgu, G., Ebinger, C.J., Maguire, P.K.H. (Eds.), *The Afar Volcanic Province within the East African Rift System*, vol. 259. *Geol. Soc., Lond., Spec. Pub.*, pp. 43–54.
- Cahen, L., 1976. Réunion de travail des 1, 2 et 3 septembre 1975: le géologie des terrains précambriens voisins du fossé tectonique occidental, spécialement dans les régions sises de part et d'autres de la partie sud du lac Kivu et du nord du lac Tanganyika au Kivu, au Rwanda et au Burundi. *Mus. Roy. Afr. Centr. Tervuren (Belg.). Dépt. Géol. Min. Rapp. Ann.* 1975, 143–170.
- Cahen, L., Ledent, D., Villeneuve, M., 1979. Existence d'une chaîne plissée Protérozoïque supérieur au Kivu oriental (Zaïre). *Données Géochronol. Relat. supergroupe l'ltombwe*. *Bull. Soc. Belge Géol* 88 (1), 71–83.
- Calais, E., d'Oreye, N., Albaric, J., Deschamps, A., Delvaux, D., Déverchère, J., Ebinger, C., Wambura, R.F., Kervyn, F., Macheyeki, A.S., Oyen, A., Saria, E., Smets, B., Stamps, D.S., Wauthier, C., 2008. Aseismic strain accommodation by dyking in a youthful continental rift, East Africa. *Nature* 456 (7223), 783–787, 11 December 2008.
- Camelbeeck, T., Vanneste, K., Alexandre, P., Verbeeck, K., Petermans, T., Rosset, P., Everaerts, M., Warnant, R., Van Camp, M., 2007. Relevance of active faulting and seismicity studies to assessments of long-term earthquake activity and maximum magnitude in intraplate northwest Europe, between the Lower Rhine Embayment and the North Sea. *Geol. Soc. Am. Spec. Pap.* 425, 193–224.
- Cornet, J., 1910. Sur la répartition des tremblements de terre dans le bassin du Congo. *Ann. Soc. Géol. Belg.* 36, B264–B269 (1908–1909).
- Corti, G., 2012. Evolution and characteristics of continental rifting: analog modeling-inspired view and comparison with examples from the East African Rift System. *Tectonophysics* 522–523, 1–33.
- Craig, T.J., Jackson, J.A., Priestley, K., McKenzie, D.M., 2011. Earthquake distribution patterns in Africa: their relationship to variations in lithospheric and geological structures, and their rheological implications. *Geophys. J. Int.* 185, 403–434.
- De Bremaeker, J.-Cl., 1956. Premières données séismologiques sur le graben de l'Afrique centrale. *Acad. Roy. Sci. Col. Bull. II* (1956–4), 762–787.
- De Bremaeker, J.-Cl., 1959. Seismicity of the West African Rift Valley. *J. Geophys. Res.* 64 (11), 1961–1966.
- De Bremaeker, J.-Cl., 1961. Séismicité du graben de l'Afrique centrale. *Mém. Inst. Géol. Univ. Louvain* 22, 99–116.
- Deelstra, H., Katihabwa, J., Waleffe, A., 1972. Les sources thermo-minérales au Burundi. *Bull. Soc. Belge. d'Etudes Géogr.* 61 (2), 233–254.
- Degens, E.T., von Herzen, R.P., Wong, H.K., Deuser, W.G., Jannasch, H.W., 1973. Lake Kivu: structure, chemistry and biology of an East African rift lake. *Geol. Rundsch.* 62, 245–277.
- Delvaux, D., Barth, A., 2010. African Stress Pattern from formal inversion of focal mechanism data. Implications for rifting dynamics. *Tectonophysics* 482, 105–128.
- Delvaux, D., Kervyn, F., Macheyeki, A.S., Temu, E.B., 2012. Geodynamic significance of the TRM segment in the East African Rift (W-Tanzania): active tectonics and paleostress in the Ufipa plateau and Rukwa basin. *J. Struct. Geol.* 37, 161–180.
- Delvaux, D., Macheyeki, A.S., Kervyn, F., Petermans, T., Verbeeck, K., Temu, E.B., 2007. Earthquake geology of the Kanda fault system (Tanganyika-Rukwa rift, SW highlands of Tanzania). *EGU general Assembly 2007*, Vienna. *Geophys. Res. Abst.* 9. <http://dx.doi.org/10.1029/2007EA00129>.
- Delvaux, D., Williamson, D., 2008. Interactions between Great lakes level change, tectonics and volcanism in the Rungwe Volcanic Province, SW highlands of Tanzania. *Acad. Roy. Sci. O.-m. Brux. Bull. Des. Séances* 54 (4), 577–600.
- Déprez, A., Doubre, C., Masson, F., Ulrich, P., 2013. Seismic and aseismic deformation along the east African Rift system from a reanalysis of the GPS velocity field of Africa. *Geophys. J. Int.* 193, 1353–1368.
- d'Oreye, N., Gonzalez, P., Shuler, A., Oth, A., Bagalwa, M., Ekström, G., Kavotha, D., Kervyn, F., Lucas, C., Lukaya, F., Osodundu, E., Wauthier, C., Fernandez, J., 2011. Source parameters of the 2008 Bukavu-Cyangugu earthquake estimated from InSAR and telesismic data. *Geophys. J. Int.* 184 (2), 934–948.
- Ebinger, C.J., 1989a. Tectonic development of the western branch of the East African rift system. *Geol. Soc. Am. Bull.* 101, 885–903.
- Ebinger, C.J., 1989b. Geometric and kinematic development of border faults and accommodation zones, Kivu-Rusizi Rift, Africa. *Tectonics* 8, 117–133.
- Ebinger, C.J., Karner, G.D., Weissel, J.K., 1991. Mechanical strength of extended continental lithosphere: constrains from the Western rift system, East Africa. *Tectonics* 10, 1239–1256.
- Fernandez-Alonso, M., 2007. Geological Map of the Mesoproterozoic Northeastern Kibara Belt. Royal Museum for Central Africa, Tervuren (Belgium) catalogue of maps and digital data. <http://www.africamuseum.be>.
- Fernandez-Alonso, M., Cutten, H., De Waele, B., Tack, L., Tahon, A., Baudet, D., Barratt, S.D., 2012. The Mesoproterozoic Karagwe-Ankole Belt (formerly the NE Kibara Belt): the result of prolonged extensional intracratonic basin development punctuated by two short-lived far-field compressional events. *Precambrian Res.* 216–219, 63–86.
- Gasthuys, P., 1939. Réseau Météorologique du Congo Belge. Guide pratique à l'usage des observateurs. Publications de la Direction Générale de l'Agriculture, de l'Elevage et de la Colonisation, Ministère des Colonies, Royaume de Belgique, p. 50.
- Giardini, D., 1999. The global seismic hazard assessment program (GSHAP) – 1992/1999. *Ann. Geofis.* 42 (6), 957–974.
- Gibowicz, S.I., Kijko, A., 1994. *An Introduction to Mining Seismology*. Academic Press, San Diego.
- Groves, A.W., 1929. Geological Survey of Uganda, Annual Report for 1929, 27.
- Gutenberg, B., Richter, C.F., 1954. *Seismicity of the Earth and Associated Phenomena*. Princeton University Press, Princeton University Press, New-York, p. 310.
- Hancock, P.L., Chalmers, R.M.L., Altunel, E., Cakir, Z., 1999. Travertines: using travertines in active fault studies. *J. Struct. Geol.* 21, 903–916.
- Hayward, N.J., Ebinger, C.J., 1996. Variations in the along-axis segmentation of the afar rift system. *Tectonics* 15 (2), 244–257.
- Herrick, P., 1959. Séismicité du Congo belge. Compilation des séismes observés aux stations climatologiques entre 1909 et 1954. *Acad. Roy. Sci. Col. Cl. Sci. Nat. méd.* 11 (5), 1–55. Mémoire in-8°. Nouvelle série.

- Jonathan, E., 1996. Some Aspects of Seismicity in Zimbabwe and Eastern and Southern Africa. M.Sc. thesis. Institute of Solid Earth Physics, Univ. Bergen, Bergen, Norway, p. 100.
- Joshi, G.C., Sharma, M.L., 2008. Uncertainties in the estimation of  $M_{\max}$ . *J. Earth Syst. Sci.* 117 (S2), 671–682.
- Kampunzu, A.B., Bonhomme, M.G., Kanika, M., 1998. Geochronology of volcanic rocks and evolution of the Cenozoic western branch of the East African rift system. *J. Afr. Earth Sci.* 23 (3), 441–491.
- Kampunzu, A.B., Lubala, R.T., Makutu, M.N., Caron, J.-P.-H., Rocci, G., Vellutini, P.-J., 1985. Les complexes alcalins de la région interlacustre à l'Est du Zaïre et au Burundi : un exemple de massifs anorogéniques de relaxation. *J. Afr. Earth Sci.* 3, 151–167.
- Kampunzu, A.B., Vellutini, P.J., Caron, L.P.H., Lubala, R.T., Kanika, M., Rumvegeri, B.T., 1983. Le volcanisme et l'évolution structurale du Sud-Kivu (Zaïre) : un modèle d'interprétation géodynamique du volcanisme distensif intracontinental. *Bull. Rech. Explor. Prod. Elf-Aquitaine* 7, 247–271.
- Kebede, F., Kulhanek, O., 1991. Recent seismicity of the east African rift system and its implications. *Phys. Earth. Planet. Inter.* 68, 259–273.
- Keir, D., Bastow, I.D., Corti, G., Mazzarini, F., Rooney, T.O., 2015. The origin of along-rift variations in faulting and magmatism in the Ethiopian Rift. *Tectonics* 34 (3), 464–477.
- Kijko, A., 2004. Estimation of the maximum earthquake magnitude,  $M_{\max}$ . *Pure Appl. Geophys.* 161, 1655–1681.
- Kijko, A., 2008. Data driven probabilistic seismic hazard assessment procedure for regions with uncertain Seimogenic zones. In: Husebye, E.S. (Ed.), *Earthquake Monitoring and Seismic Hazard Mitigation in Balkan Countries*. Springer, pp. 237–251.
- Kijko, A., Sellevoll, M.A., 1989. Estimation of earthquake hazard parameters for incomplete data files, Part I, Utilization of extreme and complete catalogues with different threshold magnitudes. *Bull. Seismol. Soc. Am.* 79, 645–654.
- Kijko, A., Singh, M., 2011. Statistical tool for maximum possible earthquake magnitude estimation. *Acta Geophys.* 59 (4), 674–700.
- Kijko, A., Smit, A., 2012. Extension of the Aki-Utsu b-Value Estimator for incomplete catalogs. *Bull. Seismol. Soc. Am.* 102 (3), 1183–1287.
- Krenkel, E., 1922. Die Bruchzonen Ostafrikas: Tectonik, Vulkanismus, Erdbeben und Schwere Anomalien. Verlag, Berlin.
- Ladmirand, H., Waleffe, A., 1991. Contribution de l'imagerie spatiale à l'étude géologique d'une partie du Maniema (Province du Kivu, Zaïre). *Bull. Soc. Géogr. Liège* 27, 229–234.
- Laerdal, T., Talbot, M.R., 2002. Basin neotectonics of lakes Edward and George, East African rift. *Palaeogeogr. Palaeoclimatol. Palaeoecol.* 197, 213–232.
- Lavreau, J., 1977. Contribution de l'imagerie spatiale à la résolution de certains problèmes géologiques au Kivu (Zaïre). *Bull. Soc. Géol. Belg.* 86 (2), 91–95.
- Lee, W., Kanamori, H., Jennings, P., Kisslinger, C., 2003. International Handbook of Earthquake and Engineering Seismology, Part B. Academic Press, p. 1000.
- Lefèvre, J., 2003. Analyse et interprétation du canevas lithostratigraphique et tectonique du synclinial de l'Itombwe (Sud-Kivu – République Démocratique du Congo) à l'aide de données satellitaires et radar. Mémoire, Université libre de Bruxelles, Dépt. Sciences de la Terre et de l'environnement, p. 109.
- Leperonne, J., 1974. Carte géologique du Zaïre au 1/2 000 000 et notice explicative. Département des Mines, Direction de Géologie, République du Zaïre, p. 67.
- Lubala, R.T., Kampunzu, A.B., Caron, J.-P., 1986. Minéralogie, pétrologie et signification géodynamique du complexe alcalin et hyperalcalin du Biega (Kivu-Zaïre). *Ann. Soc. Geol. Belg.* 109, 455–471.
- Macheyeki, A.S., Delvaux, D., De Batist, M., Mruma, A., 2008. Fault kinematics and tectonic stress in the seismically active Manyara-dodoma rift segment in Central Tanzania – implications for the east African rift. *J. Afr. Earth Sci.* 51, 163–188.
- Mavonga, T., 2007. An estimate of the attenuation relationship for the strong ground motion in the Kivu Province, Western Rift Valley of Africa. *Phys. Earth Planet. Int.* 62, 13–21.
- Mavonga, T., Durrheim, R.J., 2009. Probabilistic seismic hazard assessment for the Democratic Republic of Congo and surrounding areas. *South Afr. J. Geol.* 209, 329–342.
- McCalpin, J., 1996. Paleoseismology. In: Dworska, R., Holton, J.R. (Eds.), *International Geophysics Series* 62. Academic Press, San-Diego, p. 583.
- Meghraoui, M., Ampomah, P., Ayadi, A., Ayele, A., Bekoa, A., Bensuleman, A., Delvaux, D., El Gabry, M., ernandes, R.-M.F., Midzi, V., Roos, M., Timoulali, Y., 2016. The seismotectonic map of Africa. *Episodes* 39 (1), 9–18.
- Midzi, V., Hlatywayo, D., Chapola, L.S., Kebede, F., Atakens, K., Lombe, D.K., Turymugyendo, G., Tugume, F.A., 1999. Seismic hazard assessment in east and South Africa. *Ann. Geofis.* 42, 1067–1083.
- Morris, A., Ferrill, D.A., Henderson, D.B., 1996. Slip-tendency analysis and fault reactivation. *Geology* 24 (3), 275–278.
- Mulumba, J.-L., Delvaux, D., 2012. Pre-instrumental seismicity in Central Africa using felt seisms recorded mainly at the meteorological stations of DRC, Rwanda and Burundi during the colonial period. *EGU General Assembly 2012. Geophys. Res. Abstr.* 14. EGU2012–5931.
- Ordaz, M., Martinelli, F., Meletti, C., D'Amico, V., 2013. CRISIS2012: an Updated Tool to Compute Seismic Hazard. American Geophysical Union. Spring Meeting 2013, abstract 2013AGUSM.S52A.010.
- Passau, G., 1911. Tremblements de terre au Congo Belge (1909–1910), vol. 37. *Bull. Soc. Géol. Belg.*, p. B215 (1909–1910).
- Passau, G., 1912. Tremblements de terre au Congo Belge (1910–1911). *Ann. Soc. Géol. Belg.*, Pub. Rel. Congo Belge, Annexe au tome 39 des Annales fasc. 1, 3–4 (1911–12).
- Passau, G., 1932. La région volcanique du Sud-Ouest du lac Kivu. *Institut Royal Colonial belge. Bull.* 3 (2), 414–424.
- Passau, G., 1933. Les sources thermales de la Province Orientale (Congo Belge). *Institut Royal Colonial belge. Bull.* 4 (3), 778–814.
- Pasteels, P., Villeneuve, M., De Paepe, P., Klerkx, J., 1989. Timing of the volcanism of the southern Kivu province : implications for the evolution of the western branch of the East African Rift system. *Earth Planet. Sci. Lett.* 94, 353–363.
- Pouclet, A., 1977. Contribution à l'étude structurale de l'aire volcanique des Virunga, Rift de l'Afrique Centrale. *Rev. Géogr. Phys. Géol. Dyn.* 19, 115–124.
- Pouclet, A., 1978. Les communications entre les grands lacs de l'Afrique centrale. Implications sur la structure du rift occidental. *Mus. Roy. Afr. Centr. Tervuren (Belg.). Dépt. Géol. Min. Rapp.* Ann. 1977, 145–155.
- Pouclet, A., Bellon, H., Bram, K., 2016. The Cenozoic volcanism in the Kivu rift : assessment of the tectonic setting, geochemistry, and geochronology of the volcanic activity in the South-Kivu and Virunga regions. *J. Afr. Earth Sci.* 121, 219–246.
- Ross, K.A., Smets, B., De Batist, M., Hilbe, M., Schmid, M., Anselmetti, F.S., 2014. Lake-level rise in the late pleistocene and active subaqueous volcanism since the Holocene in Lake Kivu, East African rift. *Geomorphology* 221, 274–285.
- Rumvegeri, B.T., 1987. Le Précambrien de l'Ouest du lac Kivu (Zaïre) et sa place dans l'évolution géodynamique de l'Afrique centrale et occidentale. *Pétrologie et tectonique. Ph.D. thesis. Université de Lubumbashi, Dépt. Géologie*, p. 314, 1 carte.
- Rumvegeri, B.T., 1991. Tectonic significance of Kibaran structures in central and eastern Africa. *J. Afr. Earth Sci.* 13 (2), 267–276.
- Salée, A., Boutakoff, N., Poussin, de la Vallée, 1939. *Carte géologique de la région du Kivu, IX(1)*. Mém. Inst. Geol. Univ. Louvain, p. V.
- Sandrin, L., Marzocchi, W., 2007. A technical note on the bias in the estimation of the b-value and its uncertainty through the Least Squares technique. *Ann. Geophys.* 50 (3), 329–339.
- Saria, E., Calais, E., Stamps, D.S., Delvaux, D., Hartnady, C., 2014. Present-day kinematics of the east African rift. *J. Geophys. Res.* 119 (4), 3584–3600. <http://dx.doi.org/10.1002/2013JB010901>.
- Scholz, C.H., 2003. *The Mechanics of Earthquakes and Faulting*, 2ne Edition. Cambridge University Press, p. 471. revised.
- Scordilis, E.M., 2006. Empirical global relations converting MS and mb to moment magnitude. *J. Seismol.* 10, 225–236.
- Shcherbakov, R., Turcotte, D.L., Rundle, J.B., 2004. A generalized Omori's law for earthquake aftershock decay. *Geophys. Res. Lett.* 31, L11613. <http://dx.doi.org/10.1029/2004GL019808>.
- Shuler, A., Ekström, G., 2009. Anomalous earthquakes associated with Nyiragongo Volcano: observations and potential mechanisms. *J. Volcanol. Geotherm. Res.* 181, 219–230.
- Sieberg, A., 1932. Die erdbeben. In: Gutenberg, B. (Ed.), *Handbuch der geophysik*. Bonnrräger, Berlin 4, pp. 188–191.
- Simmons, W.C., 1929. Local Earth Tremors Recorded in February and March (1929) Connected with an Epicenter Near Ruwenzori. *Geological Survey of Uganda*, pp. 33–37. Annual Report for 1929, Part II Research Notes 1.
- Simmons, W.C., 1939. Seismology in Uganda. *Geological survey of Uganda. Bulletin* 3, 154–160.
- Smets, B., Delvaux, D., Ross, K.A., Poppe, S., Kervyn, M., d'Oreye, N., Kervyn, F., 2016. The role of inherited crustal structures and magmatism in the development of rift segments: insights from the Kivu basin, western branch of the East African Rift. *Tectonophysics* 683, 62–76.
- Stirling, M.W., Goded, T., 2012. Magnitude Scaling Relationships, GEM Faulted Earth and Regionalisation Global Components. Lower Hutt: GNS Science. GNS Science Miscellaneous Series 42. Components. Available from: [www.nexus.globalquakemodel.org/](http://www.nexus.globalquakemodel.org/).
- Sutton, G.H., Berg, E., 1958. Seismological studies of the western Rift Valley of Africa. *Trans. Am. Geophys. Union* 39 (3), 474–481.
- Sornette, D., Sornette, A., 1999. General theory of the modified Gutenberg-Richter law for large seismic moments. *Bull. Seismol. Soc. Am.* 89, 1121–1130.
- Tack, L., De Paepe, P., 1983. Le volcanisme du Sud-Kivu dans le nord de la plaine de la Rusizi au Burundi et ses relations avec les formations géologiques avoisinantes. *Mus. Roy. Afr. Centr. Tervuren (Belg.). Dépt. Géol. Min. Rapp.* Ann. 1981, 137–145.
- Tack, L., Wingate, M.T.D., De Waele, B., Meert, J., Belousova, E., Griffin, A., Tahon, A., Fernandez-Alonso, M., 2010. The 1375 Ma "Kibaran event" in Central Africa: prominent emplacement of bimodal magmatism under extensional regime. *Precambrian Res.* 180, 63–84.
- Tanaka, K., 1983. Seismicity and focal mechanisms of the volcanic earthquakes in the Virunga volcanic region. In: Hamagushi, H. (Ed.), *Volcanoes Nyiragongo and Nyamurangira. Geophysical Aspects*, Tohoku University, Japan, pp. 59–100.
- Tanaka, K., Horiuchi, S., Sato, T., Zana, N., 1980. The earthquake generating stresses in the Western rift valley of Africa. *J. Phys. Earth* 28, 45–57.
- Tedesco, D., Vaselli, O., Papale, P., Carn, S.A., Voltaggio, M., Sawyer, G.M., Durieux, J., Kasereka, M., Tassi, F., 2007. January 2002 volcanotectonic eruption of Nyiragongo volcano, Democratic Republic of Congo. *J. Geophys. Res.* 112, B09202. <http://dx.doi.org/10.1029/2006JB004762>.
- Turyomugyendo, G., 1996. Some Aspects of Seismic Hazard in the East and South African Region. M.Sc. thesis. Institute of Solid Earth Physics, University of Bergen, Bergen, Norway, p. 80.
- Twesigomwe, E., 1997. Probabilistic Seismic Hazard Assessment of Uganda. Ph.D. thesis. Dept. of Physics, Makere University, Uganda.
- Utsu, T., 1961. A statistical study on the occurrence of aftershocks. *Geophys. Mag.* 30,

- 521–605.
- Verhaeghe, M., 1963. Inventaire des gisements de calcaire, dolomies et travertins du Kivu, du Rwanda et du Burundi. Serv. Géol. Du. Congo. Mém. 3, 95.
- Villeneuve, M., 1976. Mise en évidence d'une discordance angulaire majeure dans les terrains précambriens au nord du flanc oriental du « synclinal de l'Itombwe » (Région du Kivu, République du Zaïre). C. R. Acad. Sci. Paris 282 (D), 1709–1712.
- Villeneuve, M., 1977. Précambrien du Sud du lac Kivu (Région du Kivu, République du Zaïre). Etude stratigraphique, pétrographique et tectonique. Thèse de 3<sup>ème</sup> cycle. Faculté des Sciences et Techniques de St. Jérôme, Université d'Aix Marseille III, p. 195.
- Villeneuve, M., 1978. Les centres d'émissions volcaniques du rift africain au sud du lac Kivu (République du Zaïre). Rev. Géogr. Phys. Géol. Dyn. 20, 323–334.
- Villeneuve, M., 1980. La structure du Rift Africain dans la Région du Lac Kivu (Zaïre oriental). Bull. Volc. 43, 541–551.
- Villeneuve, M., 1983. Les formations précambrrientes de Katana, au Kivu oriental (Zaïre). Mus. Roy. Afr. Centr., Tervuren (Belg.). Dépt. Géol. Min. Rapp. Ann. 1981–1982, 153–159.
- Villeneuve, M., Guyonnet-Benaize, C., 2006. Apports de l'imagerie spatiale à la résolution des structures géologiques en zone équatoriale: exemples du Précambrien au Kivu (Congo oriental). Photo-Interprétation 2006/4, 3–22. ESKA, Paris.
- Vittori, E., Delvaux, D., Kervyn, F., 1997. Kanda Fault: a major seismogenic element west of the Rukwa rift (East Africa, Tanzania). J. Geodyn. 24 (1–4), 139–153.
- Waleffe, A., 1988. Etude photogéologique du synclinorium de l'Itombwe et des régions avoisinantes au sud du 3<sup>ème</sup> parallèle sud (Kivu, Zaïre). Bull. Soc. Géol. Belg. 87 (2), 211–221.
- Walembo, K.M.A., Master, S., 2005. Neoproterozoic diamictites from the itombwe synclinorium, Kivu province, democratic Republic of Congo: paleoclimatic significance and regional correlations. J. Afr. Earth Sci. 42, 200–210.
- Wauthier, C., Cayol, V., Kervyn, F., d'Oreye, N., 2012. Magma sources involved in the 2002 Nyiragongo eruption, as inferred from an InSAR analysis. J. Geophys. Res. 117, B05411.
- Wauthier, C., Cayol, V., Poland, M., Kervyn, F., d'Oreye, N., Hooper, A., Samsonov, S., Tiampo, K., Smets, B., 2013. Nyamulagira's magma plumbing system inferred from 15 years of InSAR. Geol. Soc. Lond. Spec. Pub 380, 39–65.
- Wauthier, C., Cayol, V., Smets, B., d'Oreye, N., 2014. Magma pathways and their interactions inferred from InSAR and stress modeling at Nyamulagira volcano, D.R. Congo. Remote Sens. 2015 (7), 15179–15202. <http://dx.doi.org/10.3390/rs71115179>.
- Wauthier, C., Smets, B., Keir, D., 2015. Diking-induced moderate-magnitude earthquakes on a youthful rift border fault: the 2002 Nyiragongo-Kalehe sequence, D.R. Congo. Geochem., Geophys., Geosyst. 16 (12), 4280. <http://dx.doi.org/10.1002/2015GC006110>.
- Wayland, E., Simmons, W., 1920. Earthquakes in Uganda. Annual Rep. Geol. Dept., Entebbe, Uganda, p. 46.
- Wells, D.L., Coppersmith, K.J., 1994. Empirical relationships among magnitude, rupture length, rupture area and surface displacement. Bull. Seismol. Soc. Am. 84, 974–1002.
- Wesnousky, S.G., 2008. Displacement and geometrical characteristics of earthquake surface ruptures: issues and implications for seismic hazard analysis and the earthquake rupture process. Bull. Seismol. Soc. Am. 98 (4), 1609–1632.
- Willis, B., 1936. East African plateaus and rift valleys. In: Studies in Comparative Seismology, vol. 470. Carnegie Institution of Washington, Pub, pp. 313–328.
- Wohlenberg, J., 1968. Seismizität der ostafrikanischen Grabenzone zwischen 4°N und 12°S sowie 23°E und 40°E. Verhöll. Bayer. Komm. Intern. Erdmess. Bayer. Akad. Wiss 23, 1–95.
- Wohlenberg, J., 1969. Remarks on the seismicity of East Africa between 4°N–12°S and 23°E–40°E. Tectonophysics 8, 567–577.
- Wood, D.A., Zal, H.J., Scholz, C.A., Ebinger, C.J., Nizeré, I., 2015. Evolution of the Kivu rift, East Africa: interplay between tectonics, sedimentation, and magmatism. Basin Res. <http://dx.doi.org/10.1111/bre.12143>.
- Yang, Z., Chen, W.P., 2010. Earthquakes along the East African Rift System: a multiscale, system-wide perspective. J. Geophys. Res. 115, B12309.
- Zana, N., Hamaguchi, H., 1978. Some characteristics of aftershock sequences inn the western rift valley of Africa. Sci. Rep. Tōhoku Univ. Sér. 5, Geophys. 25 (2), 55–72.
- Zana, N., Kavotha, K., Wafula, M., 1992. Estimation of earthquake risk in Zaire. Tectonophysics 209, 321–323.
- Zielke, O., Strecker, M., 2009. Recurrence of large earthquakes in magmatic continental rifts: insights from a paleoseismic study along the laikipia–Marmanet fault, Subukia valley, Kenya Rift. Bull. Seismol. Soc. Am. 99 (1), 61–70.